Global estimates of biomass burning emissions based on satellite imagery for the year 2000

Akinori Ito and Joyce E. Penner

Department of Atmospheric, Oceanic and Space Sciences, University of Michigan, Ann Arbor, Michigan, USA

Received 6 December 2003; revised 15 March 2004; accepted 5 April 2004; published 5 June 2004.

[1] A synthesis of ground-based measurements and satellite information is described for estimating the amount of monthly averaged biomass burned in year 2000 with a spatial resolution of 1 × 1 km on a global scale. Emissions of trace gases and aerosols from open biomass burning are estimated from burned areas, fuel load maps, combustion factors, and emission factors. Burned area was quantified by using satellite data in conjunction with a fractional vegetation cover map. To account for spatial heterogeneity in the main types of vegetation within each 1-km grid cell, global fuel load maps have been developed from biomass density data sets for herbaceous and tree-covered land together with global fractional tree and vegetation cover maps. In regions with 40–60% tree cover a relationship between combustion completeness (or combustion factor) in fine fuels and tree cover based on recent field studies is implemented. In regions with <40% tree cover the combustion factor and emissions are related to global satellite-derived data for leaf area index. In regions with >60% tree cover and for coarse fuels in regions with 40–60% tree cover, average values for combustion factors and emission factors from field measurements are used. In addition to biomass burning from open vegetation fires, the emissions from biofuel burning in 2000 are estimated. Our best estimate for the global amount of burned biomass in 2000 is 5613 Tg DM yr^{-1}, of which 2814 Tg DM yr^{-1} is associated with open burning and the remainder with biofuels. The total emissions are 2290 Tg C yr^{-1} (as CO_2), 496 Tg CO yr^{-1}, 32.2 Tg CH_4 yr^{-1}, 38.0 Tg NHMC yr^{-1}, 11.5 Tg HCHO yr^{-1}, 9.2 Tg CH_3OH yr^{-1}, 21.7 Tg CH_3COOH yr^{-1}, and 38.3 Tg $PM_{2.5}$ yr^{-1}. Our estimates for CO_2, CO, and CH_4 emissions from open biomass burning combined with estimates of those from biofuel burning are in the range of the estimates constrained by chemical transport models and measurements. Our use of spatially and temporally explicit data and these comparisons to global models support the conclusion that our source map offers improvements in the emission data sets for estimating the global effects of biomass burning. *INDEX TERMS:* 0322 Atmospheric Composition and Structure: Constituent sources and sinks; 1610 Global Change: Atmosphere (0315, 0325); 0315 Atmospheric Composition and Structure: Biosphere/atmosphere interactions; 0325 Atmospheric Composition and Structure: Evolution of the atmosphere; 4805 Oceanography: Biological and Chemical: Biogeochemical cycles (1615); *KEYWORDS:* biomass burning, burned area, fuel load

Citation: Ito, A., and J. E. Penner (2004), Global estimates of biomass burning emissions based on satellite imagery for the year 2000, *J. Geophys. Res.*, *109*, D14S05, doi:10.1029/2003JD004423.

1. Introduction

[2] Biomass burning releases large amounts of trace gases and particles into the atmosphere each year. These emissions are thought to significantly influence Earth's atmosphere and climate. Therefore an accurate estimate of biomass burning emissions is required for calculations of the contribution of biomass burning to pollutant concentrations and for assessments of the contribution of biomass burning to climate change.

[3] The first estimates of emissions from biomass burning on a global scale were made over 20 years ago, and various authors have periodically provided updated estimates [*Seiler and Crutzen*, 1980; *Andreae*, 1991; *Hao and Liu*, 1994; *Liousse et al.*, 1996; *Lobert et al.*, 1999; *van der Werf et al.*, 2003]. However, the assessment of the amount of burned biomass and the associated emissions remain highly uncertain [*Crutzen and Andreae*, 1990]. The large uncertainties associated with burned biomass estimates, and in particular those associated with open burning, are caused by the uncertainty inherent in burned areas, fuel loads, combustion factors, and emission factors.

[4] Satellite remote sensing provides new data that may enable more accurate estimates of the amount of burned biomass associated with open vegetation fires. Several estimates of burned area are now available [*Grégoire et al.*, 2003; *Roy et al.*, 2002; *Simon et al.*, 2004]. The final

0148-0227/04/2003JD004423

version of the GBA-2000 data set for global burned area for the year 2000 (GBA-2000) is based on fire information derived from the VEGETATION instrument on board the Systèm Pour l'Observation de la Terre (SPOT) 4 satellite for the year 2000 [*Grégoire et al.*, 2003], although there still are uncertainties in the current burned area data [*Tansey*, 2002]. For example, A. Ito and J. E. Penner (manuscript in preparation, 2004), find that in southern Africa the range of burned areas associated with the data sets from *Grégoire et al.* [2003], *Roy et al.* [2002], and *Simon et al.* [2004] for 2000 is 155,000–830,000 km^2 for the sum of July and September, but an analysis of the spatial correlation between the GLOBSCAR and GBA-2000 burned areas concluded that the correlation is rather good in most places [*Simon et al.*, 2004].

[5] Below we examine the correspondence between burned areas defined on the basis of GBA-2000 and burned areas in which GBA-2000 is augmented by ATSR fire count areas. We also describe the uncertainties associated with the methods for estimating the fuel burned (or the fuel load) associated with different tree cover data sets (Appendix A).

[6] The amount of fuel burned has typically been estimated using a classification procedure that is based on an extrapolation of sparse data to large areas. *Scholes et al.* [1996] compared a calculation for biomass burned on the basis of conventional classification procedures to their modeled estimates. They find that their modeling method is more realistic than the classification method, in part because sparse data was extrapolated to large areas in the classification methods. Our method, like that of *Scholes et al.* [1996], is specific to the 1 × 1 km regions for which we have data. Thus, in spite of the uncertainties in fuel loads and areas burned, our method may provide more accurate estimates than older classification methods.

[7] The uncertainties associated with the amount of fuel burned in a given area result from variations in vegetation type, variations in the amount of fuel available to burn in different categories in each vegetation type, and variations in the amount of fuel combusted for a given fuel type (the combustion factor). The uncertainty in the amount of carbon held in the biomass of the forests, for example, was illustrated in a study by *Houghton et al.* [2001], who compared several estimates of forest biomass density for the Brazilian Amazon. Some of the differences among the estimates resulted from differences between actual and potential biomass density. Differences between actual and potential biomass have mainly been ascribed to changes in land-use due to human activities.

[8] Maps of actual biomass density for forested areas have been derived from the analysis of vegetation greenness measured by satellite [*Myneni et al.*, 2001; *Potter et al.*, 2001]. However, spatially distributed estimates for actual biomass density based on direct measurements are not available for all areas. Thus, in Africa, southeast Asia, and Australia, only the spatial distribution of potential biomass is available. Potential vegetation is estimated based on in situ biomass data measurements and geographical information on the variability of environmental parameters [*Brown et al.*, 1993; *Brown and Gaston*, 1995; *Barrett*, 2002]. These estimates assume that vegetation stock has reached a steady state value (the "potential value") on the basis of the assumption that there is minimum human impact, that the natural disturbed area is small relative to the total area of land, and that the disturbance is random in space and time.

[9] In order to estimate fuel loads from biomass density, representation of the heterogeneity in land cover as well as biomass productivity is crucial because fire and flood events may have changed the landscape and the accumulated fuel loads dramatically. This can be estimated using data sets that describe the percentage of tree and vegetation cover. Several global tree cover data sets are available based on remote sensing at a 1 or 0.5 km resolution [*DeFries et al.*, 2000; *Zhu and Waller*, 2001; *Hansen et al.*, 2003]. Tree cover is also related to the spatial distributions of the fuel load and influences fire characteristics.

[10] Information about emission characteristics, given the fuel and fire characteristics, has been obtained from regional field campaigns which have mainly focused on Southern Hemisphere African savannas [*Lindesay et al.*, 1996; *Swap et al.*, 2003]. Therefore we apply models for combustion and emission factors on the basis of these field campaigns in conjunction with satellite-based information on the percent tree cover (Tc) and leaf area index (LAI) to estimate the global emissions from fuel loads in regions with tree cover <60%, while averaged combustion and emission factors are used for tree cover >60%.

[11] The purpose of this paper is to develop a global map of emissions from biomass burning for the year of 2000 and to compare the total emissions thus derived with values typically used in model studies. For this purpose, satellite data sets are used to obtain burned areas and fuel distributions, while both satellite data sets and field measurements are used to determine fire characteristics for the determination of the spatial distributions and temporal variations of emissions from open vegetation fires. In section 2.1 we describe the area burned product that we use. In section 2.3 we describe our method for estimating the fuel load available to burn given the land cover classification. The fuel load is determined by the vegetation cover type (herbaceous or tree-covered) and the biomass density associated with each vegetation type as well as the litter pool and soil organic carbon. The combustion factor used for different fuel components and land cover types is described in section 2.4. In addition to burning in open vegetation fires, biofuel burning contributes to the total emissions from biomass burning. Our estimates for biofuel burning for the year 2000 are described in section 2.5. Section 2.6 describes our emission factors. Section 3 uses the available area burned estimate, the biomass density data, combustion factors, and emission factors to estimate the emissions of trace gases and particles from biomass burning and the range of amounts burned in open biomass burning associated with using different assumptions. The global distribution of biomass burning emissions is also compared to previous estimates. Finally, our estimates of CO_2, CO, and CH_4 emissions from open vegetation fires combined with estimates from biofuel burning are compared with the estimates constrained by numerical models and measurements.

2. Method for Estimating Biomass Burning Emissions

[12] The mass of burned biomass per month (M_{ijkt} kg month^{-1}) at location i, for fuel type j, within land cover type

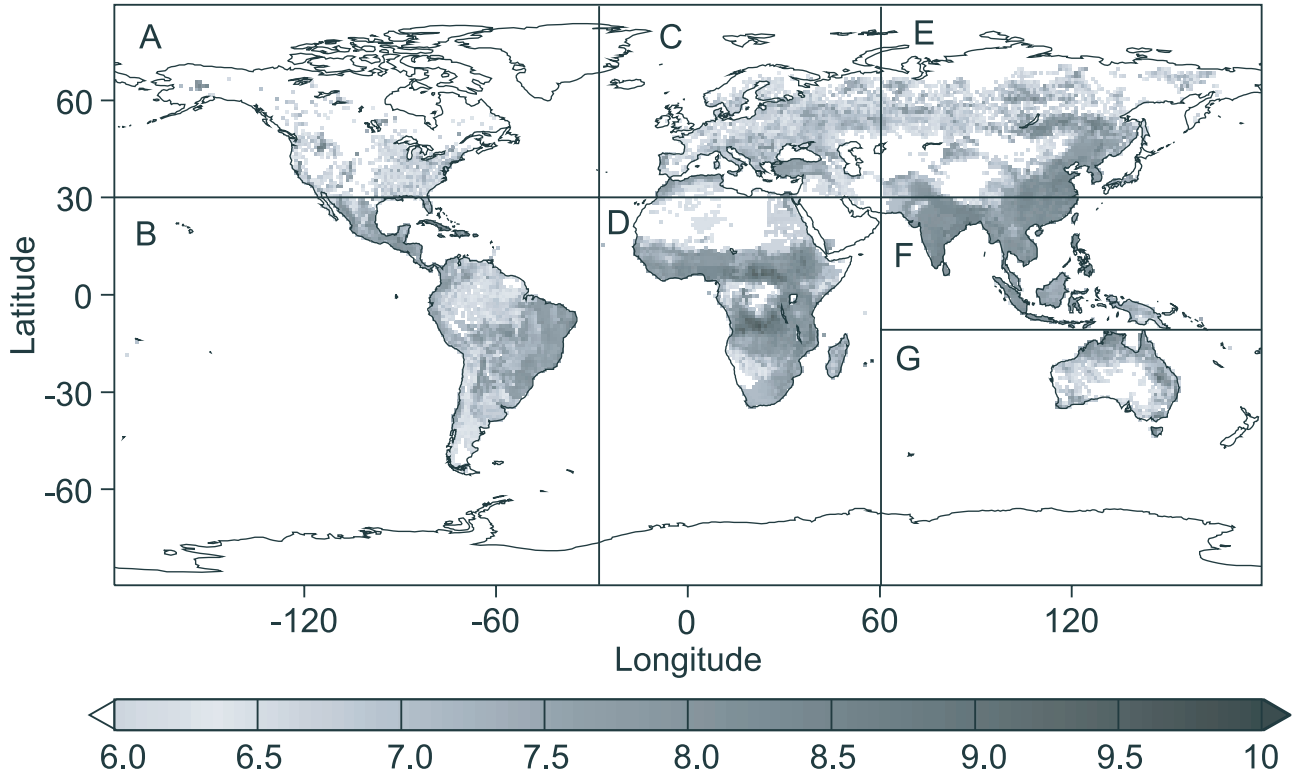

Figure 1. Global distribution of CO emissions (kg CO yr^{-1} for each 1° × 1° grid cell) from the sum of open vegetation fires and biofuel fires on a $\log_{10}$ scale. The regions associated with different biomass density data sets (regions A through G) are also shown. See color version of this figure in the HTML.

k, and for month t in open vegetation fires can be described by the following equation [*Seiler and Crutzen*, 1980],

$$[M]_{ijkt} = [A]_{it} \times [B]_{ijkt} \times [CF]_{ijkt}, \quad (1)$$

where A is the burned area per month at location i (m^2 $month^{-1}$), B is the fuel load (kg m^{-2}) expressed on a dry weight (DM) basis for the fuel class j within each grid i, and CF is the fraction of available fuel which burns (the combustion factor). As we explain below, CF is a function of the fuel class in all land cover types, but it is a function of time and location for fine fuels in grasslands, and it is a function of location for fine fuels in woodlands. We have written the more general form above showing the variation of CF with time and location for all land cover types and fuel classes because in future work we hope to be able to add these features. In this work, fuel loads are developed for herbaceous- and tree-covered land areas in each 1 × 1 km grid of burned area (see section 2.3). We differentiate between three types of land cover (grasslands, woodlands, and forests) which are defined on the basis of the tree cover fraction, and we use separate methods for calculating combustion factors in these three land cover types. The fuel classes j that we consider include fine and coarse living tissue, fine and coarse litter, and soil organic carbon, but different classes are burned depending on the land cover type based on observed fire behavior. The amount of biomass burned together with the mode of burning (flaming or smoldering) is used to estimate emissions of carbon dioxide (CO_2), carbon monoxide (CO), methane (CH_4), nonmethane hydrocarbons (NMHC), formaldehyde (HCHO), methanol (CH_3OH), acetic acid (CH_3COOH), and particulate matter less than 2.5 μm in diameter ($PM_{2.5}$).

2.1. Area Burned

[13] The determination of the monthly burned area was based on new satellite remote sensing techniques and procedures [*Grégoire et al.*, 2003]. The GBA-2000 data were developed from a coalition of researchers working to develop estimates of burned area in different regions using the SPOT-VEGETATION S1 (1-day composite) imagery. Each group was responsible for the validation of their algorithm in their region. The global data for the year 2000 were provided on a 1 × 1 km grid resolution each month. Each cell was specified as either burned ("1") or not burned ("0"). Because the data that we use for developing emissions estimates varies from region to region, we distinguish the following six regions: Canada, Alaska and the United States of America north of 30°N (region A), Central and South America and the United States of America south of 30°N (region B), Europe, European Russia, Africa north of 30°N, and the Middle East (region C), sub-Saharan Africa (region D), Asian Russia and Asia north of 30°N (region E), Asia south of 30°N (region F), and Australia (region G) (see Figure 1). An assessment of the accuracy of the classification tree in GBA-2000 shows that it performed very well at classifying the unburned areas in southern Africa (the southern part of region D) [*Silva et al.*, 2003]. However, it should be noted that small fires and under-story fires beneath thick forest canopy are not always detected in the GBA-2000 algorithms. In contrast, the Along

Table 1. Summary of Data Sets and Parameterizations Used in the Estimation of Emissions From Open Vegetation Fires

Name[a]	Sources	Method	Year
IGBP[b]	*Loveland et al.* [2000]	unsupervised clustering	1992–1993
FVC[c]	*Zeng et al.* [2000]	NDVI comparison with IGBP	1992–1993
TC1	*DeFries et al.* [2000]	linear mixture model + classification	1992–1993
TC2	*Zhu and Waller* [2001]	modified linear mixture model	1995–1996
TC3	*Hansen et al.* [2003]	regression model	2000–2001
CF1	see Tables 3 and 4 and section 2.4.1	compilation of measurements	
CF2	*Hély et al.* [2003]	exponential model + TC2	1995–1996
CF3	*Hoffa et al.* [1999]	linear regression model + LAI[d]	2000–2000
EF1	see Table 5 and section 2.6.1	compilation of measurements	
EF2	see Table 6 and section 2.6.2	linear regression model + LAI	2000–2000

[a]Abbreviations are as follows: TC, tree cover; CF, combustion factor; EF, emission factor.
[b]IGBP land cover map.
[c]Fractional vegetation cover map.
[d]Leaf area index from *Myneni et al.* [1997].

Track Scanning Radiometer (ATSR) fire algorithm can detect small hot spots of order 0.1 ha for detection of a 600°K fire and 0.01 ha for an 800°K fire [*Arino and Melinotte*, 1998], although the total ATSR fire count is underestimated because it only detects fires at night and when the satellite is overhead [*Arino and Plummer*, 2001]. In this work, ATSR fire counts are used to compensate for the possible underestimation of fires in GBA-2000 by assuming that the entire 1 × 1 km grid cell in which ATSR detects a fire is subject to burning even though the fires that are detected may be smaller than this grid cell [*Arino and Plummer*, 2001]. This may overestimate the total area burned for the smaller fires detected by ATSR. Nevertheless, the use of this data set allows us to examine the possible errors in the GBA-2000 data set in different regions.

[14] Because the values of the burned area occurrence were given as either a "0" or "1" in each 1 × 1 km area, the burned area detected by remote sensing includes any land covered by vegetation as well as any bare ground within those cells. Therefore we accounted for the effects of bare ground on the area burned using a separate data set for each 1 × 1 km grid,

$$[A]_{it} = [A']_{it} \times [Fc]_i, \quad (2)$$

where A' is the burned area detected by satellite and Fc is the fractional area covered by vegetation. The data for Fc were derived from a fractional vegetation cover set Fc' that was available from *Zeng et al.* [2000] and the fractional tree cover data set (see section 2.2).

2.2. Vegetation Cover Data Set

[15] Tree cover (TC) data were examined for three different data sets (referred to as TC1, TC2, and TC3), which were derived from different sources and methods (see Table 1). The first data set (TC1) used the AVHRR satellite data set for 1992–1993 [*DeFries et al.*, 2000], the second (TC2) used AVHRR for 1995–1996 [*Zhu and Waller*, 2001], and the third data set (TC3) used the Moderate-Resolution Imaging Spectroradiomter (MODIS) satellite data set for 2000–2001 [*Hansen et al.*, 2003]. TC1, which was a prototype of TC3, used a linear mixture model based on spectral signatures of end-members or pure pixels of forest, grassland, and bare ground training, with some adjustments in regions where results were known to be biased [*DeFries et al.*, 2000]. TC2 (developed for the Forest Resources Assessment (FRA) 2000 report [*Saket*, 2001]) was produced using temporal compositing of AVHRR NDVI and a modified mixture analysis. TC3 employs continuous training data over the whole range of tree cover as opposed to a linear mixture model [*Hansen et al.*, 2003]. Our area burned data set (GBA-2000) represents the year 2000, while the MODIS (TC3) tree cover data refers to 31 October 2000 to 9 December 2001. It is inevitable that the fractional tree cover in the tree cover data set derived from MODIS has been reduced compared to the actual tree cover for the GBA-2000 time period because some areas covered by trees were burned from January 2000 to October 2000. However, the TC2 data set probably represents higher tree cover than that for the year 2000 since it was developed from data for earlier time periods. Appendix A provides a comparison of the tree-covered areas by region in TC1, TC2, and TC3. However, only some of the differences represent real differences associated with changes in tree cover due to burning, and some of the differences in tree cover data sets from different time periods are due to differences in instrumentation and methods (and thus represent inaccuracies in one or more of the data sets). Since the land cover determined for TC3 represents a new approach based on the MODIS instrument, it should provide an improved description of tree cover [*Hansen et al.*, 2002]. Version 3.0.0 of the TC3 data set has on average about 15% less tree-covered area than does TC2 (see Appendix A). However, we could not use the TC3 data set with the burned area data set for 2000 because it includes most of the burned area from the year 2000 and would therefore underestimate the total fuel load that was burned in 2000. Therefore we used TC2 since it is at least prior to the time of burning associated with GBA-2000. However, our estimates of biomass burned are uncertain to the extent that this data set (as well as the burned area data set) is uncertain.

[16] The available global 1-km fractional vegetation cover (Fc) was derived from the Advanced Very High Resolution Radiometer (AVHRR) normalized difference vegetation index (NDVI) data for 1992–1993 on the basis of the annual maximum NDVI value for each pixel in comparison with the NDVI value that corresponds to 100% vegetation cover for each IGBP land cover type [*Zeng et al.*, 2000]. One might suppose that trees and herbaceous cover could have grown into areas of bare ground between 1992–1993

and 2000. However, areas that were previously covered by vegetation might also have been cleared. Such concerns are of particular importance because 1992–1993 was an El Nino year, while 2000 was a La Nina year. However, we have no high-resolution data set that might be used to correct for these temporal changes. Moreover, we wish to determine the fractional area covered by herbaceous cover as the difference between the fractional area covered by vegetation and the fractional area covered by trees. So one should examine the possibility that either or both of the data sets contain errors. The differences between our data set for vegetation cover that has been corrected for tree cover (Fc) and that provided by *Zeng et al.* [2000] (Fc') are examined in Appendix A. There we show that the differences associated with the use of these two different data sets for fractional vegetation is not large (only 1% on a global average basis, see Appendix A). Because the TC2 tree cover data is closer in time to our period of analysis, the tree cover data set was assumed to be more accurate than the fractional vegetation cover data set. Therefore the fractional herbaceous cover was derived from the difference between the fractional vegetation cover (Fc') from *Zeng et al.* [2000] and the fractional tree cover (Tc) but is constrained to be greater than zero. To summarize, Fc used in equation (2) is derived from the following equation,

$$[Fc]_i = [Tc]_i + [Hc]_i, \tag{3}$$

where Hc is the fractional area covered by herbaceous vegetation derived from

$$[Hc]_i = [Fc']_i - [Tc]_i, \tag{4}$$

where $Hc \geq 0$. We note that Fc may be larger than Fc' if $Fc' - Tc$ is less than zero.

2.3. Fuel Load

[17] Global fuel load maps were produced from the existing vegetation cover and biomass density data sets. The biomass density data sets are described in sections 2.3.1 and 2.3.2. The vegetation data sets are supplemented by a litter pool data set and a soil organic carbon data set. The litter pool data set is described in sections 2.3.3 and 2.3.4. The soil organic carbon data set is described in section 2.3.5. The model for the fuel load subject to burning in each land cover type is described in section 2.3.6.

2.3.1. Living Tree Biomass Density Data Sets

2.3.1.1. Temperate and Boreal Forests (Regions A, C, and E)

[18] *Myneni et al.* [2001] estimated biomass carbon pool maps for temperate and boreal forests in the Northern Hemisphere north of 30°N from the patterns of greenness deduced from AVHRR NDVI. These authors regressed NDVI against above-stump and total biomass for different types of forests that was deduced from inventory data of stem wood volume from 171 provinces in six countries. *Myneni et al.* [2001] used the 1 km global International Geosphere-Biosphere Programme (IGBP) land cover data set, which was produced through a continent-by-continent unsupervised classification of 1 km AVHRR NDVI composites with ancillary data analysis in 1992–1993 [*Loveland et al.*, 2000] to determine the forest area in each region. These data sets provided a method to determine the total above-stump woody biomass for northern temperate and boreal forests in regions A, C, and E. These data of the carbon pools were available at an 8 km spatial resolution for the time period averaged over 1981–1999.

[19] The carbon pools from the original total woody biomass data were converted back to total woody biomass by multiplying by 2 since a conversion factor of 0.5 was used in the work of *Myneni et al.* [2001]. The total woody biomass includes above-stump woody biomass, stumps, and roots but excludes foliage.

[20] Since the living stumps and roots would not burn appreciably, the above-stump woody biomass was estimated from the total woody biomass using the average ratio of above-stump woody biomass to total woody biomass in North America and Eurasia from the original forest inventory data used by *Myneni et al.* [2001] [*Liski and Kauppi*, 2000]. These were calculated to be 87 and 79% in North America and Eurasia, respectively.

[21] The biomass of leaves was estimated from the above-stump biomass and the average ratios of foliage to above-stump wood, which were measured to be 10.3 and 2.6% for evergreen and deciduous forests in U.S. mid-Atlantic region forests, respectively [*Jenkins et al.*, 2001]. The median ratio of 6.5% between evergreen and deciduous forests was used for the leaf biomass of mixed forests. Forest areas of the three different vegetation types (evergreen, deciduous, and mixed forests) were available on a 1 km grid from the IGBP land cover map [*Loveland et al.*, 2000].

[22] These data could underestimate the actual biomass density in forests in the 1 km grid cells that are available from GBA-2000 data set if the tree cover for the 1 km grid resolution is heterogeneous and thus larger (in any given 1 km grid) than the average tree cover in the 8 km grid. Therefore we determined the total biomass in each 8 km grid by multiplying the biomass density from *Myneni et al.* [2001] by the total forest area (which was assumed to be the sum of broad leaf forests, needleleaf forests, mixed forests, and woody savannas) as determined using the IGBP land cover types [*Loveland et al.*, 2000]. This definition of forest corresponds to that used by *Myneni et al.* [2001] and was defined as any land cover type in the IGBP land cover data base with tree cover >30%. Then this biomass was distributed to the fractional tree-covered areas as determined by TC2 within each 1 km grid cell. Using this procedure, the total amount of biomass determined by *Myneni et al.* [2001] is preserved, and the horizontal variation in each 1 × 1 km grid box is represented.

2.3.1.2. Central and South America (Region B)

[23] For the Amazon, estimates of the spatial distribution of biomass density from spatially distinct measurements have not been developed. However, *Potter et al.* [2001] used the vegetation greenness index, NDVI, derived from AVHRR as a multiyear input for net primary production to a terrestrial ecosystem model to predict the forest biomass. The subsequent biomass density data set is available at an 8 km resolution for the early 1990s [*Potter et al.*, 2001]. This data set, called the NASA Ames Research Center Amazon Ecology (AME) mapping data set, is composed of maps of aboveground leaf and woody biomass for the Amazon region associated with region B. Outside of the Amazon the aboveground woody biomass density data sets

for each country in 2000 were obtained from the FRA 2000 main report [*Saket*, 2001] (see section 2.3.1.5).

2.3.1.3. Tropical Africa and Asia (Regions D and F)

[24] Data from measurements were not available to directly estimate the spatially distributed actual biomass density of the forests in regions D and F. However, the horizontal distribution of biomass density can be accounted for by combining the tree cover data set (TC2) and potential biomass density data. The spatial distribution of potential biomass density of forests with a minimum of 10% crown cover for Africa (region D) and southern Asia (region F) was estimated by *Brown et al.* [1993] and *Brown and Gaston* [1995] using a weighted overlay of four input parameters: mean annual precipitation, a climatic index, elevation and slope, and soil depth and texture class. Weighting factors were adjusted through an iterative process by comparing the model results to measured biomass densities in undisturbed regions. These spatial distributions of potential biomass in Africa and southern Asia were obtained from the Carbon Dioxide Information Analysis Center (CDIAC) at 5 and 3.75 km resolution, respectively. We converted the potential carbon densities in forests for southern Asia (which included both aboveground and belowground carbon) back to aboveground biomass densities on the basis of data sets obtained from CDIAC and the procedure described in the work of *Brown et al.* [1993]. We then separated the aboveground forest biomass into the biomass of leaves and above-stump woody biomass using the average ratios of foliage to above-stump tree biomass of 9.3 and 2.5% for evergreen and deciduous forests, respectively, determined for mid-Atlantic forests in the United States [*Jenkins et al.*, 2001] because no adequate data were available that were specific to areas of Africa and Asia. The median ratio of 5.9% between evergreen and deciduous forests was used for the leaf biomass of mixed forests.

[25] In addition to the above procedures, some countries in region *F* were not available from the *Brown et al.* [1993] data set. In these areas, country-specific data for 2000 were obtained from the FRA 2000 main report [*Saket*, 2001] (see section 2.3.1.5).

2.3.1.4. Australia (Region G)

[26] The spatial distribution of the steady state potential biomass density in Australia (region G) was available at 0.05 degree resolution for forests, woodlands, and shrublands [*Barrett*, 2002]. The method used to estimate this distribution employed an iterative adaptive search method of optimization to minimize C-cycle model data deviations and maximize consistency between estimated model parameters and all available observations. The available biomass data characterized the aboveground fine and coarse tissue living biomass and aboveground fine and coarse tissue litter.

2.3.1.5. Additional Forest Biomass Density Data Set (Regions B and F)

[27] Aboveground woody biomass density data sets for each country in 2000 were obtained from the FRA 2000 main report [*Saket*, 2001]. This estimate of woody biomass in forests is based on inventory reports and additional data adjustments when needed. These country-averaged biomass density data were used for estimates of biomass density, where the data sets in sections 2.3.1.2 and 2.3.1.3 were unavailable. As above, the biomass density of leaves was estimated from the aboveground woody biomass and the average ratio of foliage to above-stump wood measured in U.S. mid-Atlantic region forests [*Jenkins et al.*, 2001].

Table 2. Comparison of Biomass Density (kg DM m^{-2}) in Grasslands

	Gill et al. [2002]	Long-Term Mean[a]	Year 2000[b]
Average	0.291	0.244	0.425
Minimum	0.080	0.070	0.023
Maximum	0.933	0.582	1.338
Standard deviation	0.156	0.124	0.265

[a]Biomass density calculated from the equation (5) and the long-term mean of precipitation obtained at each location [*Gill et al.*, 2002].

[b]Biomass density calculated from the equation (5) and annual precipitation interpolated at each location from the global data set available on a 0.5° × 0.5° grid [*Roads et al.*, 2003].

2.3.2. Herbaceous Cover Biomass Density

[28] Biomass density data for herbaceous cover (i.e., shrubs and grass) is derived from an estimate for the maximum standing biomass (excluding trees) in savannas. The following equation of biomass density (kg DM m^{-2}) versus annual rainfall (mm) has been applied to obtain the amount of carbon released during fires in Guinea savannas [*Menaut et al.*, 1991]:

$$[\text{biomass density}]_{it} = 4.9 \times 10^{-4} \times [\text{annual rainfall}]_{it} - 0.58. \quad (5)$$

This equation was used in this work to estimate the maximum biomass in herbaceous cover. Interannual variability in the aboveground production of herbaceous biomass was accounted for by using the monthly precipitation data from the Global Precipitation Climatology Project (GPCP) of the Laboratory for Atmospheres, NASA Goddard Space Flight Center (GSFC). This data set is available at a resolution of 0.5° × 0.5° and was used for annual rainfall from 1999 to 2000 [*Roads et al.*, 2003].

[29] To evaluate the use of equation (5) globally, we used data sets for the biomass density from 42 grassland sites distributed around the world [*Gill et al.*, 2002]. The average biomass density compiled by *Gill et al.* [2002] together with that estimated from equation (5) using the local long-term measurements of annual precipitation from these 42 sites is shown in Table 2. We also show the estimated biomass density for 2000 at these sites on the basis of the annual precipitation interpolated from the GPCP data set. The average biomass density calculated from the long-term mean precipitation at each location (0.24 ± 0.12 kg DM m^{-2}) is in good agreement with the measured biomass density (0.29 ± 0.16 kg DM m^{-2}). The average biomass density estimated from the precipitation in 1999–2000 is higher (i.e., 0.42 kg DM m^{-2}) but is associated with the interannual variation at each site. We conclude that this is a reasonable method for estimating the maximum herbaceous cover biomass density. We note, however, that this biomass density only accounts for the density associated with grasses. Furthermore, grass density would decrease as tree cover increases, but in woodlands and forests, including this effect would be only a small perturbation to our fuel burn estimates. In areas with $Tc < 40\%$, only fine fuels generally burn [*Scholes et al.*, 1996; *Hély et al.*, 2003; *Hansen et al.*, 2003], and our fuel estimate therefore accounts for these fuels and their variation with rainfall amounts.

2.3.3. Fine Litter Fuel Load

[30] Litter pool (also referred to as forest floor mass or litter mass) is defined as recently fallen litter and decomposing organic matter above the mineral soil. *Matthews* [1997] developed an estimate for the fine litter pool associated with each vegetation type from a compilation of biomass density measurements for different vegetation types. We distributed the pools from the *Matthews* [1997, Table 6] model 1D to the *Matthews* [1983] global ecosystem map, which is available at a resolution of $1^\circ \times 1^\circ$. This procedure maintains the total litter pool that was originally developed by *Matthews* [1997]. An alternate procedure would be to distribute these litter pools to the 1×1 km ecosystem map developed by *Loveland et al.* [2000], which was based on the ecosystem map of *Olson* [1994]. However, there is no one-to-one correspondence between these two ecosystem maps. Therefore we opted to maintain the methods developed by *Matthews* [1997]. These values of fine litter mass were used to estimate fine litter fuel loads in all areas except for Australia, where the estimates from *Barrett* [2002] were used.

2.3.4. Coarse Woody Debris Fuel Load

[31] *Matthews* [1997] employed the technique outlined in the work of *Harmon and Hua* [1991] to estimate the pool of coarse woody debris (CWD) on the basis of measured relationships between the CWD pools and live wood biomass. *Harmon and Hua* [1991] report ratios of CWD to live wood biomass of 5% for tropical rain forests, shrublands, and grasslands and ~20–25% for subtropical, temperate, and boreal forests. Here we used the live tree biomass data set derived here and the *Harmon and Hua* [1991] ecosystem ratios of CWD to live tree biomass with the ecosystem map from *Matthews* [1983] to estimate CWD. These values of CWD were used to estimate fuel loads in all areas except for Australia, where the estimates from *Barrett* [2002] were used.

2.3.5. Soil Organic Carbon

[32] The average soil organic carbon (SOC) density (kg C m^{-2}) for peat soils for 0–50 cm depth range and for 0–100 cm depth range were derived by *Batjes* [1996]. He used version 1.0 of the World Inventory of Soil Emission Potential Database (WISE) profile database, linked to a $0.5 \times 0.5^\circ$ raster version of the FAO Soil Map of the World to derive SOC [*Batjes*, 1996]. We used this SOC for peat soils together with an average burned depth of 51 cm on the basis of the field measurements reported by *Page et al.* [2002]. It should be noted, however, that the depth of peat burned varied between 25 and 85 cm for the measurements analyzed by *Page et al.* [2002], so that the use of a single average depth for this factor introduces a degree of uncertainty. The value of SOC from peat soils for the first 51 cm depth was calculated to be 47.1 kgC m^{-2}, which was interpolated from the average for peat soils for 0–50 cm and 0–100 cm reported by *Batjes* [1996] using a log-log model for the vertical distribution of SOC [*Jobbágy and Jackson*, 2000]. Only SOC that was in regions of peat soils based on the map derived by *Zobler* [1986] was burned because the SOC in mineral soils is not subject to combustion in fires. The peat soil map from *Zobler* [1986] was compiled on a 1° grid on the basis of the FAO Soil Map of the World.

2.3.6. Fuel Load Subject to Burning

[33] Fire behavior can be described by the following five types of fire:

[34] 1. Low-intensity surface fires of aboveground fuels.

[35] 2. Burning of tree-covered areas associated with land conversion to pasture and maintenance of pastures.

[36] 3. High-intensity fires of felled trees.

[37] 4. High-intensity crown fires of living trees.

[38] 5. Smoldering fires (i.e., oxygen-starved inefficient consumption of the fuel) of dead and downed logs and ground-layer carbon (e.g., lichen, moss, and organic soil).

[39] We use these categories of fire types to define the fuel load subject to burning in each 1×1 km grid. In order to represent the fuel characteristics for each type of fire, we classified land cover type into three classes, forests, woodlands, and grasslands, on the basis of the percentage of tree canopy cover following *Hansen et al.* [2000]. Forests were defined as those regions with greater than 60% tree cover, woodlands were defined as those regions with 40–60% tree cover, and grasslands were defined as those areas with less than or equal to 40% tree cover. These categories are consistent with definitions in the work of *Matthews* [1983] and *Hansen et al.* [2000].

[40] In general, fires in savanna regions (which are classified as grasslands in our land cover types) are low-intensity fires that do not consume the biomass of live shrubs and trees [*Shea et al.*, 1996; *Hoffa et al.*, 1999]. Moreover, living and dead wood more than 5 cm in diameter are not traditionally counted as part of the burned fuel load in these regions [e.g., *Scholes et al.*, 1996]. Therefore we conservatively assumed that the living tree components, and coarse woody debris were not burned in grasslands.

[41] In woodlands, however, large-diameter woody fuels are consumed by pasture-maintenance burns [*Kauffman et al.*, 1998; *Guild et al.*, 1998] and by the residual smoldering fires after a flaming front passes [*Bertschi et al.*, 2003a] but may not be consumed in less intense fires. Different assumptions about the inclusion of large-diameter woody fuels in the fuel loads subject to burning lead to the different estimates for emissions. Therefore we considered four scenarios in estimating the long-term emissions in woodlands that differentiate between scenarios with and without residual smoldering combustion of large logs and with and without felled trees that result from pasture maintenance burns. First, we define the residual smoldering factor (RSF) as the fraction of large wood that is burned as a result of smoldering combustion. In scenarios 1 and 3 (Sc1 and Sc3), we assume that only the area associated with the ATSR fire counts is subject to long-lasting fires which consume the large logs that are part of the CWD (RSF = 1), while in scenarios 2 and 4 (Sc2 and Sc4), all of the fires in all burned areas consume the CWD. In addition, we define a tree felled factor (TFF). In Sc1 and Sc2 the TFF is equal to 1, meaning that all trees in areas subject to fires are assumed to have been felled, so that the coarse woody fuels include both the CWD defined above and the living trees which have all been assumed to have been felled prior to the burn. Sc3 and Sc4 correspond to the assumptions for area subject to residual smoldering as in Sc1 and Sc 2, but TFF was set to 0, which means that no trees are assumed

to have been felled, so that the only coarse fuels that burn are the CWD defined in section 2.3.4.

[42] To sum up, we defined four different scenarios:

[43] 1. Sc1: RSF = 1 and TFF = 1 in only the grid cells where ATSR fire counts are detected.

[44] 2. Sc2: RSF = 1 TFF = 1 in all grid cells where burning is detected.

[45] 3. Sc3: RSF = 1 in only grid cells where ATSR fire counts are detected, while TFF = 0 in all grids.

[46] 4. Sc4: RSF = 1 and TFF = 0 in all grid cells.

[47] In forested regions we assumed that the fires detected by GBA-2000 were either high-intensity crown fires or that trees had been felled for slash-burn fires. Thus the fires in forested areas could consume part of the above-stump living trees and the CWD. Therefore our fuel load included these components. In addition, for Sc2 and Sc4, the belowground soil organic carbon was included as a fuel in all burned areas, while for Sc1 and Sc3 it was only included where ATSR hot spots were detected.

[48] On the basis of this model, for each land cover type (grassland, woodland, or forest), biomass density data were represented for the two vegetation cover types (herbaceous and tree-covered) within each 1 km grid by the following five categories: aboveground fine and coarse living tissue biomass, aboveground fine and coarse litter, and SOC. The biomass density data for each living fuel type were derived from available biomass data sets for each region, as described above. We developed living tree biomass data for woody and leafy parts separately (see sections 2.3.1), while estimates for the living biomass density of herbaceous cover by month were based on the relationship between rainfall and in situ biomass density measurements (section 2.3.2). Data sets for fine litter, CWD, and SOC were also available for all of the regions (sections 2.3.3–2.3.5).

[49] In order to account for the horizontal allocation of the biomass, fractional tree and herbaceous-covered vegetation areas were separately estimated to derive the average biomass fuel load in each 1 km grid cell. The biomass densities of tree-covered regions were allocated to the fractional area associated with trees. The biomass density data of herbaceous-covered areas predicted from the relationship between rainfall and biomass density were distributed in the fraction of area not covered by trees and not counted as bare ground. Thus the average fuel load ($[B]_{it}$) in each 1 × 1 km cell can be calculated from the fuel loads for each fuel type j, which include those for herbaceous cover ($[B]_{iht}$), the fine litter pool fuel load ($[B]_{if}$), the CWD ($[B]_{ic}$), the living wood fuel load ($[B]_{iw}$), the living leaf fuel load ($[B]_{il}$), and belowground fuel load (or SOC) ($[B]_{ib}$) in each land cover type k according to the following.

[50] Grasslands ($[Tc]_i \leq 40\%$) (i.e., land cover type $k = 1$):

$$[B]_{it} = [Hc]_i \times [B]_{iht} + [Tc]_i \times [B]_{if}. \quad (6)$$

Woodlands ($40\% < [Tc]_i \leq 60\%$) ($k = 2$):

$$[B]_{it} = [Hc]_i \times [B]_{iht} + [Tc]_i \times \{[B]_{if} + [B]_{il} + RSF \times ([B]_{ic} + TFF \times [B]_{iw})\}. \quad (7)$$

Table 3. Combustion Factors for Fine and Coarse Fuels in Forests From Various Sources

Study	Fine Fuels[a]	Coarse Fuels[b]	Average Aboveground Fuels
Fearnside et al. [1993]	1.00	0.26	0.29
Fearnside et al. [1999]	0.97	0.32	0.43
Fearnside et al. [2001]	0.68	0.26	0.30
Carvalho et al. [1998]	0.88	0.14	0.20
Carvalho et al. [2001]	0.92	0.26	0.33
Guild et al. [1998]	0.95	0.47	0.51
Araújo et al. [1999]	0.83	0.13	0.20
Graça et al. [1999]	0.96	0.29	0.36
Combustion factor[c]	0.90 ± 0.10	0.27 ± 0.09	0.33 ± 0.10
RSD,[d] %	12	40	32

[a]Litter and leaves.
[b]Wood such as branches and trunks.
[c]The average CF for fine fuels and coarse fuels were separately used in this study.
[d]Relative standard deviation.

Forests ($60\% < [Tc]_i$) ($k = 3$):

$$[B]_{it} = [Hc]_i \times [B]_{iht} + [Tc]_i \times ([B]_{if} + [B]_{il} + [B]_{ic} + [B]_{iw} + RSF \times [B]_{ib}), \quad (8)$$

where TFF represents whether the trees are felled or not.

2.4. Combustion Factor

[51] The combustion factor (CF) is the fraction of biomass exposed to fire that is actually consumed. The CF is mainly determined by fuel type, fuel spatial arrangement, and fuel moisture content. The CF for all fuel types in forests assumed an average combustion factor and is described below in section 2.4.1. The CF for fine fuels (herbaceous fuel and fine litter) in woodlands depends only on the tree cover fraction (section 2.4.2), while the CF for fine fuels in grasslands is a dynamic combustion factor that depends on the moisture condition of the fuel (section 2.4.3).

2.4.1. Combustion Factor in Forests

[52] The average CF for herbaceous vegetation in forests is assumed to be 0.99 as determined for 13 field measurements for grassland fires in Africa [*Shea et al.*, 1996]. The average CF for fine litter and leaves and for coarse woody debris and the coarse fuels associated with living trees in forests was estimated from field measurements of CF obtained from detailed studies in tropical rain forests as summarized in Table 3 [*Fearnside et al.*, 1993, 1999, 2001; *Carvalho et al.*, 1998, 2001; *Guild et al.*, 1998; *Araújo et al.*, 1999; *Graça et al.*, 1999]. Typically, the original forests were slashed and burned by property owners at these sites toward the end of the dry season. Therefore we have assumed that living trees are felled in tropical forests prior to burning. The CF for this vegetation was determined from the percentage difference in biomass before and after burning for fine fuels (such as litter and leaves) and for coarse fuels (such as wood) separately. These CFs for fine and coarse fuels are presented in Table 3. The combustion factor for fine dry fuels from these studies is relatively high at 0.90 ± 0.10. In contrast, the CF for coarse fuels is only 0.27 with a high relative standard deviation of 40%. Since the fuel loads for fine and coarse fuels are differentiated in

our model, the average CF for fine fuels and coarse fuels were separately used to estimate the biomass burned in forests.

[53] Because crown fires in forests are not differentiated from slash fires in forests in this work, the average CF summarized in the third column in Table 3 was compared with those measured in other fires. From the data in Table 3 we find a weighted average CF of 0.33 ± 0.10 for total aboveground fuels in tropical slash-burn fires. This is similar to the CF found in high consumption severity fires in the Alaskan boreal forest [*French et al.*, 2002]. This agreement indicates that a CF of order 0.3 may be representative of the large-area fires detected by remote sensing in most regions. Although this consumption factor may be too high in extratopical forests if fires are not as severe as those summarized by *French et al.* [2002], most of the area detected in GBA-2000 may refer to severe fires because the GBA-2000 data set excludes most single pixel fire areas [*Gregoire et al.*, 2003]. We also note that the ATSR fire counts did not add substantial area to that already included in GBA-2000 (see section 3) in extratropical forests (regions A, C, and E). All of the soil organic matter between 0 and 51 cm depth in the peat soils of forested regions was also treated as fuel. The CF for SOC was assumed to be 36.5% from the average value in high consumption severity fires reported by *French et al.* [2002].

[54] The CF is influenced by the fuel conditions (moisture content and packing density). Methods for determining biomass burning that predict these conditions have the advantage of representing such parameters within each ecosystem and may therefore yield more accurate estimates of CF. However, because the amount of data available to estimate CF is so limited, we feel that the simple approach used here (using constant combustion factors) is justified at the present time, though we hope to replace this method in the future.

2.4.2. Combustion Factor in Woodlands

[55] Because the percentage tree cover controls the fuel type distribution in each region and thus influences fire propagation and intensity, *Hély et al.* [2003] developed an empirical relationship between CF and Tc on the basis of dry season fires in Zambia and South Africa during the SAFARI-92 campaigns and a fire in the Etosha National Park of Namibia. Here we apply this relationship (designated CF2 in Table 1) to herbaceous fuels, leaves, and fine litter in woodlands:

$$[CF]_{ij} = \exp\left(-0.013 \times [Tc]_i\right) \quad \left(40\% < [\mathrm{Tc}]_i \leq 60\%\right), \qquad (9)$$

where the fuel types *j* include the fine litter fuels as well as herbaceous cover and leaves.

[56] Because this model was developed for fuel loads such as grass, litter, and small woody debris in southern Africa at the end of dry season, in applying it throughout the season, we are assuming that regional fuels in the burning seasons are sufficiently dry to ignore the dependency of CF on moisture content.

[57] We used an average combustion factor for CWD in woodlands on the basis of the measurements (which were for coarse fuels with diameter > 2.55 cm) summarized in Table 4 [*Kauffman et al.*, 1998; *Guild et al.*, 1998]. Thus an average value of 30% was used for our estimates of the burning of coarse woody debris in woodlands.

Table 4. Combustion Factors for Coarse Fuels in Woodlands From Various Sources

Study	Study Areas	Coarse Fuels[a]
Kauffman et al. [1998]	Rondônia	0.09
Kauffman et al. [1998]	Rondônia	0.28
Kauffman et al. [1998]	Pará	0.61
Guild et al. [1998]	Pará	0.20
Combustion factor[b]		0.30 ± 0.20
RSD,[c] %		66

[a]Wood debris larger than 2.55 cm diameter.
[b]Average ± standard deviation.
[c]Relative standard deviation.

2.4.3. Combustion Factor in Grasslands

[58] The combustion factor in grasslands can be determined from the percentage of green grass to total grass (PGREEN) since this accounts for the seasonal and spatial variation in CF [*Hoffa et al.*, 1999]. In this work, PGREEN for 2000 was estimated from the leaf area index (LAI) derived by *Myneni et al.* [1997]. Myneni et al. determined the LAI from the maximum normalized difference vegetation index (NDVI) value in global composites of the NOAA/NASA Pathfinder AVHRR land data set. The derivation of LAI used an algorithm that incorporates results from a three-dimensional radiative transfer model and a six biome classification scheme [*Myneni et al.*, 1997]. The global data sets of monthly averaged LAI at 16 km resolution were available from 1999 to 2000.

[59] It was assumed that the maximum LAI of the monthly averages in the growing season represented the total grass available to burn within a season. Then the parameter PGREEN was estimated from the ratio of the LAI of the monthly averages to the maximum monthly average LAI over the growing season. The relationship between PGREEN and CF derived in the work of *Hoffa et al.* [1999] (designated CF3 in Table 1) was applied to herbaceous fuels and fine litter in grasslands:

$$[\mathrm{CF}]_{it} = -213[\mathrm{PGREEN}]_{it} + 138 \quad \left([\mathrm{Tc}]_i \leq 40\%\right). \qquad (10)$$

We limited the value of CF to the range from 0.44 to 0.98 to avoid any extrapolation beyond the measured values for grassland fires.

2.5. Biofuel Emissions for 2000

[60] Although the focus of this paper is the biomass burning from open vegetation fires, estimates for biofuel emissions for 2000 are included to complete the emission inventory from biomass burning. The global distribution of biofuel emissions for the developed countries was estimated from the Food and Agricultural Organization (FAO) Statistical Database (FAOSTAT) data, while those for the developing countries followed the methods used by *Yevich and Logan* [2003] to extrapolate for their inventory (which was developed for 1985) to the year 1995.

2.5.1. Developed Countries

[61] The consumption of wood fuel in cubic meter and of charcoal in tones for developed countries was estimated on the basis of FAOSTAT databases for the production, import, and export of these fuels (see http://apps.fao.org). The mass

Table 5. Emission Factors (Gram Species per Kilogram Dry Matter Burned) From Various Sources[a]

Species	CO_2	CO	CH_4	NMHC	HCHO	CH_3OH	CH_3COOH	$PM_{2.5}$
Woodland	1613	65	2.3	3.4	1.06	1.17	2.42	5.4
CWD in woodlands	1454	158	23.2	8.3 [b]	3.48	8.09	8.43	13.1[b]
Tropical forest	1580	104	6.8	8.1	1.4	2	2.1	9.1
Extratropical forest	1569	107	4.7	5.7	2.2	2	3.8	13
SOC in forests	1436	112	9	6.0–8.7[c]	0.49	1.07	1.43	9.80–13.6[c]
Fuel wood in developed	1550	78	6.1	7.3	3.52	3.61	8.12	7.2
Charcoal in developed	2661	200	6.2	2.7	0.73	1.24	3.2	9
Fuel wood in developing	1467	70	4.5	7.3	3.52	3.61	8.12	7.2
Charcoal in developing	2740	230	8	2.7	0.73	1.24	3.2	9
Dung	1010	60	2.7	7	1.4	2	0.8	3.9
Crop residues	1192	86	4.6	7	1.4	2	0.8	3.9
Charcoal making in Africa	1593	254	39	2	0	0.16	0.98	0
Charcoal making in T. America	966	162	32	2	0	0.16	0.98	0
Charcoal making in T. Asia	1403	133	18	2	0	0.16	0.98	0

[a]From *Andreae and Merlet* [2001], *Bertschi et al.* [2003a, 2003b], *Yevich and Logan* [2003], and *Yokelson et al.* [2003].
[b]EF determined from the EF for NMHCs for woodlands summarized by *Andreae and Merlet* [2001] and the ratio of EF for CO for CWD in woodlands [from *Bertschi et al.*, 2003a] and for CO in woodlands from *Andreae and Merlet* [2001].
[c]Range is that from extratropical forest to tropical forest. The EF was determined from the EF for NMHCs for forests summarized by *Andreae and Merlet* [2001] and the ratio of EF for CO for SOC in forests [from *Bertschi et al.*, 2003a] and for CO in forests from *Andreae and Merlet* [2001].

of burned biomass per year (kg yr^{-1}) was estimated using the density, moisture content, and ash content given in the FAOSTAT statistics (see http://apps.fao.org). The burning of these fuels is distributed within each country by population only during the winter [*Liousse et al.*, 1996].

2.5.2. Developing Countries

[62] We used data provided by *Yevich and Logan* [2003] and their methods for estimating biomass burning in the developing world for 1995 from the emissions for 1985 to calculate estimates for biofuel burned in developing countries for 2000. It should be noted that while Yevich and Logan included the biofuels consumed in Japan as part of Asia's total, their estimates in Japan were excluded from this work since Japan is included as part of the inventory of biofuels from developed countries. Following *Yevich and Logan* [2003], to extrapolate the emissions for fuelwood burning, charcoal burning, charcoal production, crop residue used for domestic fuels, and dung used as biofuels from 1985 to 2000, we used population changes from the United Nations Population Database (see http://esa.un.org/unpp/). Crop production changes from FAO were used to estimate crops burned for agroindustrial use (see http://apps.fao.org).

2.6. Emission Factors

[63] The emissions of gases and particles per month (kg species $month^{-1}$) are calculated from

$$[Q(X)]_{it} = \sum \left([M]_{ijkt} \times [\mathrm{EF}(X)]_{ijkt} \right), \qquad (11)$$

where X is chemical species and EF is the emission factor in gram species per kilogram of dry matter burned. The emissions factors for fuels in woodlands and forests as well as biofuel burning assumed an average emission factor, designated EF1 in Table 1. In grasslands, to account for the type of combustion (e.g., flaming and smoldering fires), we used an approach based on relating the emission factor to the combustion efficiency of the fuel (designated EF2 in Table 1). We also compared these results for grasslands to results that used the average emission factors for savanna and grasslands recommended in the work of *Andreae and Merlet* [2001] and results that used the regression estimates measured by *Yokelson et al.* [2003].

2.6.1. Emission Factors Used for Biofuels, Woodlands, and Forests

[64] Measurements of EFs in different regions were reviewed and tabulated by *Andreae and Merlet* [2001]. The averaged EFs for CO_2, CO, CH_4, NMHC, and $PM_{2.5}$ for savanna and grasslands from Table 1 in that paper were applied to our woodland land cover type (except for the emission factors associated with smoldering fires of coarse fuels), while those for HCHO, CH_3OH, and CH_3COOH were taken from recent measurements [*Yokelson et al.*, 2003]. Those from tropical forests from *Andreae and Merlet* [2001, Table 1] were applied to our forests except for the smoldering fires of SOC in regions B, D, F, and G, while those from extratropical forests such as boreal and temperate forests were applied to forests in regions A, C, and E. Emission factors for CO_2, CO, CH_4 HCHO, CH_3OH, and CH_3COOH from smoldering fires of coarse fuels (RSF = 1) in woodlands and SOC in forests were taken from those measured for logs and organic soils, respectively [*Bertschi et al.*, 2003a]. Emission factors for CO_2, CO, CH_4, NMHC, and $PM_{2.5}$ for biofuel burning and charcoal burning in developed countries are taken from *Andreae and Merlet* [2001] and applied to wood fuel and charcoal burning, while those for HCHO, CH_3OH, and CH_3COOH are from *Bertschi et al.* [2003b]. Emission factors for CO_2, CO, and CH_4 for biofuels in the developing countries are taken from *Yevich and Logan* [2003], those for HCHO, CH_3OH, and CH_3COOH are from *Bertschi et al.* [2003b], and those for NMHC, and $PM_{2.5}$ are from *Andreae and Merlet* [2001]. These EFs are summarized in Table 5.

2.6.2. Emission Factors in Grasslands

[65] Emission factors are expected to change with season owing to the nature of the combustion. Fuels are moister during the early part of the season, causing more smoldering combustion. The amount of smoldering combustion can be estimated from the modified combustion efficiency (MCE), which is defined as the ratio of CO_2 emitted to the sum of CO and CO_2 because emissions of the products of incomplete combustion, such as CO, are relatively larger during

Table 6. Comparison of Average Emission Factors (Gram Species per Kilogram Dry Matter Burned) for Grasslands

Species	This Study	*Andreae and Merlet* [2001]	*Yokelson et al.* [2003]
CO_2, g-CO_2 kg-DM^{-1}	1694	1613	1703
CO, g-CO kg-DM^{-1}	69.4	65	71.5
CH_4, g-CH_4 kg-DM^{-1}	2.16	2.3	2.19
NHMC, g-NMHC kg-DM^{-1}	3.17	3.4	
HCHO, g-HCHO kg-DM^{-1}	1.47	0.26–0.44	1.06
CH_3OH, g- CH_3OH kg-DM^{-1}	1.09	1.3	1.17
Hac[a] g-CH_3COOH kg-DM^{-1}	2.37	1.3	2.42
$PM_{2.5}$, g-$PM_{2.5}$ kg-DM^{-1}	4.54	5.4	

[a]Acetic acid.

smoldering combustion [*Ward and Radke*, 1993]. The MCE can be related to PGREEN by [*Hoffa et al.*, 1999]:

$$[\mathrm{MCE}]_{it} = -0.286[\mathrm{PGREEN}]_{it} + 1.019 \quad \left([\mathrm{Tc}]_i \le 40\%\right). \quad (12)$$

The range for MCE in grasslands was limited to 0.908–0.966.

[66] Here we used a linear regression to relate compound-specific emission factors to MCE on the basis of field measurements for savanna and grassland fires in Africa, Australia, and Alaska [*Hurst et al.*, 1994a, 1994b; *Andreae et al.*, 1996; *Ward et al.*, 1996; *Goode et al.*, 2000; *Shirai et al.*, 2003; *Sinha et al.*, 2003; *Yokelson et al.*, 2003]. Thus our linear model is based on data from a wide variety of independent fire measurements varying from tropical to boreal zone fuels. The number of measurements (n) ranges from 11 to 27.

$$[\mathrm{EF}(\mathrm{CO_2})]_{it} = 2134[\mathrm{MCE}]_{it} - 311.2 \quad \left(n = 27, R^2 = 0.42\right) \quad (13)$$

$$[\mathrm{EF}(\mathrm{CO})]_{it} = -1134[\mathrm{MCE}]_{it} + 1135 \quad \left(n = 27, R^2 = 0.99\right) \quad (14)$$

$$[\mathrm{EF}(\mathrm{CH4})]_{it} = -51.8[\mathrm{MCE}]_{it} + 50.253 \quad \left(n = 26, R^2 = 0.74\right) \quad (15)$$

$$[\mathrm{EF}(\mathrm{NMHC})]_{it} = -45.96[\mathrm{MCE}]_{it} + 46.358 \quad \left(n = 17, R^2 = 0.34\right) \quad (16)$$

$$[\mathrm{EF}(\mathrm{PM_{2.5}})]_{it} = -86.67[\mathrm{MCE}]_{it} + 85.985 \quad \left(n = 11, R^2 = 0.55\right) \quad (17)$$

[67] When the emission factors of the three species, CO_2, CO, and CH_4, were measured for the same fires by both gas chromatography on canister samples (CG/C) [*Sinha et al.*, 2003] and airborne Fourier transform infrared spectroscopy (AFTIR) [*Yokelson et al.*, 2003], the AFTIR values were used in this work. The proportion of carbon per unit biomass fuel is generally taken to be 0.45 [*Andreae and Meret*, 2001], but different authors use different values in different studies. We note that if a consistent value of 0.45 is used to recalculate the EFs for all studies then the correlation coefficient (R^2) for the relationship between the CO_2 emission factor and MCE increases from 0.42 to 0.93, but here we followed the recommendations of each author for the proportion of carbon per unit biomass. Additionally, there were two extraneous data points for NMHC in the CG/C values that significantly reduced R^2 to under 0.5. It is unclear whether these outliers are a result of measurement error or are due to variations in the NMHC content of the smoke, although the EF of CO_2 for these two data points are smaller than the AFTIR values. All of the reported values were used for the regression estimates at this point. The emission factor equations for HCHO, CH_3OH, and CH_3COOH used the relationships between EF and MCE given in the work of *Yokelson et al.* [2003].

2.6.3. Comparison of Dynamic and Average Emission Factors in Grasslands

[68] In addition to the dynamic EF for grasslands described above (section 2.5.2), we also examined the use of the average EF determined by *Andreae and Merlet* [2001] and the average measured EF from *Yokelson et al.* [2003] in grasslands. Table 6 shows the globally and seasonally averaged estimates of the EFs for CO_2, CO, CH_4, NMHC, HCHO, CH_3OH, CH_3COOH, and $PM_{2.5}$ for grassland fires. The average emission factors from the compilation of *Andreae and Merlet* [2001] and average of the measurements reported by *Yokelson et al.* [2003] are also shown. As shown there, the emission factors for CO_2, CO, CH_4, NMHC are in good agreement (to within 10%), but the emission factor for HCHO, which was based on the data of *Yokelson et al.* [2003], is outside the range determined by *Andreae and Merlet* [2001]. These results suggest that the modeled relationship between EF and MCE can be used to estimate the emissions for grasslands globally but that further work may be needed to define the appropriate emission factor for HCHO.

3. Results and Discussion

[69] The area burned (10^3 km^2 yr^{-1}) in grasslands, woodlands, and forests for each region is presented in Table 7. The values in parentheses in this table represent the percentage of the total area burned that was estimated from only the GBA-2000 data set. More than 98% of the total burned area on a global scale was estimated from the GBA-2000 data set. However, only 86 and 64% of the total area burned in the forested areas of regions A and B, respectively, was estimated from GBA-2000. Apparently, there is an underestimation of burnt areas in Canadian forests and

Table 7. Areas Burned (10^3 km^2 yr^{-1}) for Grasslands, Woodlands, and Forests for Each Region

Regions	Grasslands	Woodlands	Forests	Total
A	15 (90)[a]	3 (92)	15 (86)	33 (88)
B	88 (90)	5 (85)	29 (64)	123 (84)
C	116 (97)	4 (94)	14 (89)	134 (96)
D	1571 (99)	342 (99)	260 (99)	2173 (99)
E	150 (96)	19 (96)	82 (94)	251 (96)
F	60 (95)	9 (94)	17 (89)	86 (93)
G	266 (98)	50 (98)	23 (96)	339 (98)
Total	2266 (98)	433 (99)	440 (94)	3139 (98)

[a]Values in parentheses represent the percentage of the total area burned from GBA-2000. The total is the sum of the area from GBA-2000 and the ATSR fire count data set.

Table 8. Fuel Load (kg DM m^{-2}) for Grasslands, Woodlands, and Forests in Areas Exposed to Fire for Each Region[a]

Regions	Grasslands	Woodlands	Forests
A	0.26	1.06–2.44[b] (0.85–1.04)[c]	8.91–9.02[d]
B	0.49	1.70–7.89 (0.75–1.52)	15.93–15.94
C	0.28	1.25–2.48 (1.15–1.33)	7.39–7.48
D	0.35	0.99–9.54 (0.88–1.65)	14.83–14.84
E	0.23	1.40–2.87 (1.34–1.58)	7.13–7.63
F	0.54	1.95–8.73 (1.39–2.53)	16.07–16.09
G	0.45	1.03–6.16 (0.84–1.94)	14.23–14.23
Average	0.37	1.34–5.73 (1.03–1.65)	12.07–12.18

[a]The area exposed to fire is the burned area that is covered by herbaceous vegetation and trees in grasslands, woodlands, and forests.
[b]Scenarios 1–2.
[c]Values in parentheses represent scenarios 3 and 4.
[d]Scenarios 1–2. This range is the same as that for Sc3–Sc4 since in Sc2 and Sc4 in forests SOC is assumed burned in all areas in which fires are burned, whereas in Sc1 and Sc3, only the SOC in those regions in which ATSR fires are detected is burned.

Central and South America in GBA-2000. Since we added the entire 1 × 1 km grid box associated with the ATSR fire count data, our estimates for burned area in the places where only ATSR fires are detected may be too large. However, the GBA-2000 underestimate is only partly compensated for by the ATSR fire data since these data only recorded fires that were present at night. Clearly, our estimates of emissions associated with regions A and B should be considered more uncertain than those from other regions.

[70] Annual averages of aboveground fuel loads in the regions exposed to fire are compared for the land cover types for each region in Table 8. The average fuel load for grasslands calculated from seven regions (0.37 ± 0.12 kg DM m^{-2}) is within the estimated range from measurements (0.29 ± 0.16 kg DM m^{-2}) in Table 2. The regional averages in woodlands in region B for Sc2, 7.89 kg DM m^{-2}, is the highest value among the various scenarios because coarse woody fuels are assumed to be efficiently consumed in Sc2. However, this value is comparable to the total measured above ground biomass fuel load for slash fires in woodlands in the Brazilian Amazon which ranged from 5.3 to 11.9 kg DM m^{-2} [*Kauffman et al.*, 1998; *Guild et al.*, 1998]. As discussed previously, Sc2 represents a scenario which assumes that all trees are felled and burned as in slash fires in woodlands. The regional averages for forests in the tropical areas such as B, D, and F range from 14.8 to 16.0 kg DM m^{-2}, which is within the range of measurements for fuel loads in closed forests quoted in the work of *Hao et al.* [1990] (4.9–32.8 kg DM m^{-2}).

Table 9. Average Combustion Factors for Grasslands, Woodlands, and Forests Fires in Areas Exposed to Fire for Each Region

Regions	Grasslands	Woodlands	Forests
A	0.59	0.47–0.37[a] (0.51–0.46)[b]	0.44–0.44[a]
B	0.59	0.39–0.32 (0.51–0.40)	0.32–0.32
C	0.63	0.49–0.39 (0.51–0.48)	0.51–0.51
D	0.81	0.49–0.32 (0.52–0.41)	0.32–0.32
E	0.73	0.49–0.39 (0.50–0.47)	0.50–0.49
F	0.73	0.61–0.37 (0.73–0.54)	0.33–0.33
G	0.67	0.48–0.33 (0.52–0.39)	0.33–0.33
Average	0.68	0.49–0.35 (0.54–0.45)	0.39–0.39

[a]Range represents scenarios 1 and 2.
[b]Values in parentheses represent scenarios 3 and 4.

Table 10. Biomass Burned (Tg DM yr^{-1}) for Grasslands, Woodlands, and Forests Fires for Each Region

Regions	Grasslands	Woodlands	Forests	Total
A	2	2–3[a] (1–2)[b]	58–58[a]	62–64 [a] (61–62)[b]
B	25	4–14 (2–3)	148–148	177–187 (176–177)
C	21	3–4 (2–3)	51–52	74–76 (74–75)
D	438	168–1037 (157–234)	1229–1230	1835–2705 (1824–1902)
E	26	13–21 (13–14)	292–306	331–352 (330–345)
F	24	10–28 (9–12)	91–91	125–143 (124–127)
G	80	25–101 (22–38)	107–107	211–287 (208–224)
Total	616	224–1207 (206–305)	1975–1991	2814–3814 (2797–2912)

[a]Range represents scenarios 1 and 2.
[b]Values in parentheses represent scenarios 3 and 4.

[71] Annual averages of CF for grasslands, woodlands, and forests are presented for each region in Table 9. The regional averages of CF in woodlands for Sc2, 0.32–0.39, are the lowest values among the various scenarios because the coarse woody fuels have the smallest CF, and these are largest in Sc2. The regional averages of CF for forests in extratropical regions such as A, C, and E are larger than those in the tropical areas such as B, D, and F because fine fuels make up a larger fraction of the total fuel in extratropical regions.

[72] The annual amounts of biomass burned in open vegetation fires are summarized for each region in Table 10. The differences in biomass burned between Sc1 and Sc2 are 983 Tg and 16 Tg for woodlands and forests, respectively. Although the amount of large woody fuel available for burning is highly uncertain, scenario 1 may provide the most reasonable estimates based on a comparison of the amounts burned in South Africa from this scenario to measurements, as well as a comparison of fuel loads with data, and a comparison of combustion factors with measurements (A. Ito and J. E. Penner, manuscript in preparation, 2004). However, we present this range because our conclusions for southern Africa may not apply to all locations. In particular, in South America, Sc2 may be the best choice because of the slash-burn practices that are prevalent there.

[73] Annual areas and amounts of biomass burned are compared to other studies in Table 11. Our emission estimates are relatively low mainly because of the lower amounts of area burned in tropical America and Asia [*Hao et al.*, 1990; *van der Werf et al.*, 2003]. To the extent that small area fires or under-story fires are missed, the combined GBA-2000 and ATSR products may still underestimate the true area and amounts burned.

[74] The annual emission from open vegetation fires and biofuel burning for each compound estimated here is summarized in Table 12. Our source strengths from biomass burning can be compared with the estimates from model studies, which have used surface fluxes of atmospheric trace gases that provide a reasonable comparison of their model results with atmospheric observational data. Our estimates of CO_2, CO, and CH_4 emissions from open

Table 11. Comparison of Annual Areas Burned (10^3 km^2 yr^{-1}) and Biomass Burned in Open Vegetation Fires (Tg DM yr^{-1}) for Different Studies

Study	Africa	Australia	T. America	T. Asia	NH
		Burned Areas, $10^3 km^2 yr^{-1}$			
This work	2173[a]	339[b]	23[c]	86[d]	417[e]
Hao et al. [1990]	4640		1590	240	
Hurst et al. [1994a]		870			
Liousse et al. [1996]	3440				
Barbosa et al. [1999]	2880–5160[f]				
Lavoué et al. [2000]					24–438[g]
Russell-Smith et al. [2003]		418			
van der Werf et al. [2003]	2820	1180	1040	390	
		Biomass Burned in Open Vegetation Fires, Tg DM yr^{-1}			
This work[h]	1835–2705	211–287	177–187	125–143	466–492
This work[i]	1824–1902	208–224	176–177	124–127	466–482
Hao et al. [1990]	2820	420	1360	351	
Hao and Liu [1994]	2290	290	1500	413	
Hurst et al. [1994a]		210			
Liousse et al. [1996]	1690				
Barbosa et al. [1999]	700–2170				
Lobert et al. [1999]					640
Lavoué et al. [2000]					66–700
NGGIC [2002]		150[j]			
Shirai et al. [2003]		260			
van der Werf et al. [2003]	2290	330	1510	489	

[a]Region D.
[b]Region G.
[c]Region B.
[d]Region F.
[e]Sum of regions A, C, and E.
[f]Range refers to the fraction of pixel assumed burned for the time period from 1985 to 1991.
[g]Range of burned areas during 1960–1997.
[h]Scenarios 1–2.
[i]Scenarios 3–4.
[j]Emission estimates are based on an average of emissions for the years 1995 to 1998 [*NGGIC*, 2002].

biomass burning combined with estimates of emissions from biofuel use yields a range from 2.29 to 2.69 Pg C (as CO_2), from 495 to 654 Tg CO, and from 32.1 to 55.2 Tg CH_4 from our different scenarios, while the estimates constrained by numerical models and measurements are from 1 to 3 Pg C (as CO_2) [*Tans et al.*, 1993; *Siegenthaler and Sarmiento*, 1993; *Schimel et al.*, 1996; *Heimann and Maier-Reimer*, 1996; *Waring et al.*, 1998; *Kicklighter et al.*, 1999], from 370 to 1250 Tg CO [*Warneck*, 1988; *Bergamaschi et al.*, 2000a, 2000b; *Holloway et al.*, 2000], and from 25 to 70 Tg CH_4 [*Fung et al.*, 1991; *Warneck*, 1988; *Prather*, 1996]. As a result, our emission estimates for the products of complete combustion (PCC) from this bottom-up approach in our lowest cases (Sc1 and Sc3) are in the middle of the range determined from these top-down approaches, while those for the products of incomplete combustion (PIC) are in the lowest part of this range. However, the estimated emissions of the PIC in our highest cases (Sc2 and Sc4) are in better agreement with the middle of the range from the model studies. These results may imply that the fraction of smoldering combustion should be larger than we estimated in Sc1 and Sc3. Figure 1 summarizes the global distribution of CO emissions on a $\log_{10}$ scale from the sum of open vegetation fires and biofuel burning at a resolution of $1^\circ \times 1^\circ$, using the Sc1 scenario as summarized in Table 12. The global distribution of CO emissions strongly depends on the global map of area burned, while the strength of CO

Table 12. Emissions From Open Vegetation Fires and Biofuel Burning in 2000

Species	Open Vegetation Fires	Biofuels[a]	Biofuels[b]	Total
CO_2, Pg-C yr^{-1}	1.23–1.63[c] (1.22–1.23)[d]	0.05	1.01	2.29–2.69[c] (2.29–2.28)[d]
CO, Tg-CO yr^{-1}	264–421 (263–363)	8	224	496–654 (495–595)
CH_4, Tg-CH_4 yr^{-1}	15.7–38.7 (15.7–36.6)	0.6	15.8	32.2–55.2 (32.1–53.1)
NMHC, Tg-NMHC yr^{-1}	18.8–27.1 (18.7–24.1)	0.8	18.5	38.0–46.4 (38.0–43.3)
HCHO, Tg-HCHO yr^{-1}	4.3–7.7 (4.2–6.7)	0.4	6.9	11.5–15.0 (11.5–14.0)
CH_3OH, Tg-CH_3OH yr^{-1}	1.1–9.1 (1.1–8.0)	0.4	7.7	9.2–17.1 (9.2–16.1)
Hac,[e] Tg-CH_3COOH yr^{-1}	6.9–15.2 (6.9–13.1)	0.9	13.9	21.7–29.9 (21.6–27.8)
$PM_{2.5}$, Tg-$PM_{2.5}$ yr^{-1}	22.1–35.3 (22.0–30.5)	0.8	15.4	38.3–51.5 (38.2–46.7)

[a]Biofuel burning from the developed countries.
[b]Biofuel burning from the developing countries.
[c]Scenarios 1–2.
[d]Values in parenthesis represent scenarios 3 and 4.
[e]Acetic acid (CH_3COOH).

emissions is influenced by other factors. In future studies, this emissions data set will be tested using a global atmospheric chemistry transport model.

4. Conclusions

[75] The global and seasonal emissions of trace gases and aerosols from open biomass burning have been estimated on the basis of spatial and temporal variations in fuel consumption and fire behavior. In this paper we have reported the global emissions from vegetation fires as well as biofuel burning for the year 2000.

[76] As we show in Appendix A, the selection of the tree cover data set has important implications for the amount of biomass burned. The three data sets for tree cover that we examined differ because of different years analyzed, different remote sensing classification techniques, and different satellite instrument characteristics. Similar differences in fractional vegetation data sets may also occur (see Appendix A). The most recent tree cover data set, TC3, unfortunately does not apply to the year that we analyzed because the time period for this data set overlaps and is later than that of the area-burned data set. Clearly, these data sets, as well as that for burned area, need further validation and should be made available on an annual basis if biomass burning estimates are to improve. Furthermore, the errors associated with the estimation of tree cover in these data sets need to be quantified.

[77] The accuracy of biomass density data sets also needs to be established. In this paper we had to rely on different techniques for estimating biomass density in tree-covered areas. Improving these estimates will require improved and representative ground-based measurements.

[78] Empirically derived equations for CF and EF for grasslands were successfully combined with the monthly averaged LAI derived from satellite data to estimate global biomass burning emissions from grasslands. We derived equations for the dependence of EF on the modified combustion efficiency (MCE) on the basis of data sets from field measurements in Africa, Australia, and Alaska. Our results show that the averaged emission factors for CO_2, CO, CH_4, NMHC are in good agreement (to within 10%) with the average emission factors summarized by *Andreae and Merlet* [2001], but that the emission factor for HCHO is outside the range determined by *Andreae and Merlet* [2001]. A temporally and spatially dynamic treatment for the CF and EF is preferable to a treatment that uses a constant CF and EF (as was done in woodlands and forests) because it accounts for the seasonal variation in CF and EF due to variations in the moisture content of the fuel. Clearly, it would be desirable to incorporate treatments for the CF and EFs that would account for variations associated with moisture content.

[79] Our emissions estimates are lower than most previous studies. In particular, our estimates are lower than the estimates provided by *Hao et al.* [1990] and *Hao and Liu* [1994], which are broadly used in global atmospheric chemistry transport models. The main reason for our smaller estimates for open burning emissions is the lower burned area in tropical regions. To account for the underestimates in the burned area in tropical regions from the GBA-2000, we supplemented the areas burned with the area associated with the detection of hot spots by ATSR. Nevertheless, our burned areas in tropical America and tropical Asia are significantly smaller than those in other studies. Although our results are smaller than the biomass burned in the inventory of *Hao et al.* [1990], when we add our new estimates for biofuel burning, we are in the same range as the emissions of CO_2, CO, and CH_4 emissions constrained by numerical models and measurements. These results and the fact that we have temporally and spatially resolved estimates support the conclusion that our source map for emissions from biomass burning offers improvements over methods that are based on classification techniques. Our study revealed that there are important differences in the estimates of biomass burning depending on the amount of smoldering combustion that is assumed. Moreover, the comparison of our estimates of the emissions of the PIC with those from model studies may imply that the fraction of smoldering combustion should be larger than our best estimates for Sc1. Future studies should quantify further the effects of residual smoldering of CWD and SOC on estimates of global biomass fire emissions.

[80] In our approach the use of spatially and temporally explicit data sets to represent the heterogeneity in land cover

Table A1. Comparison of Tree-Covered Areas (10^3 km^2 yr^{-1}) for Each Land Cover Type for Different Tree Cover Maps for Each Region

Region	TC1	TC2	TC3[a]	Average	RSD,[b] %
			Grasslands		
A	758	444	1315	839	53
B	1186	333	1852	1124	68
C	588	193	931	571	65
D	1383	807	1994	1395	43
E	1007	210	1518	911	72
F	597	283	802	561	47
G	357	187	365	303	33
Total	5876	2457	8777	5704	55
			Woodlands		
A	1309	620	1397	1109	38
B	1549	278	916	915	70
C	714	361	829	634	38
D	1869	852	859	1193	49
E	1269	668	1421	1119	36
F	693	367	818	626	37
G	182	174	56	137	51
Total	7586	3319	6296	5733	38
			Forests		
A	2674	4617	1866	3052	46
B	5787	7577	5196	6187	20
C	1365	3091	1147	1868	57
D	1832	3069	1654	2185	35
E	2290	6252	1335	3292	79
F	1917	2898	2130	2315	22
G	207	297	138	214	37
Total	16,072	27,802	13,467	19,114	40
			Total Over All Land Cover Types		
A	4741	5681	4578	5000	12
B	8523	8189	7964	8225	3
C	2667	3645	2907	3073	17
D	5084	4727	4507	4773	6
E	4565	7130	4274	5323	30
F	3207	3549	3750	3502	8
G	746	658	559	654	14
Sum	29,534	33,578	28,540	30,551	9

[a]This analysis used the 3.0.0 version of the TC3 data set.
[b]Relative standard deviation.

has been explored, whereas most previous global emission inventories were based on a classification method with data compiled using a variety of data from national reports together with a statistical approach for the amount of material burned. Consequently, the emission model developed here is specific to the time period analyzed and has the advantage of accounting for explicit spatial and temporal variations. Global atmospheric chemistry transport models will be used to study the relative contribution of open biomass burning emissions to current and future air pollution and to estimate the radiative forcing associated with anthropogenic emissions of gases and aerosols.

Appendix A

[81] As discussed in the text, there are several possible sources of error in our analysis, including errors associated with having data sets that refer to years other than 1999–2000 and errors associated with the analysis that produced the data set (owing to differences in the remote sensing classification techniques and different satellite instrument characteristics). Here we provide tables that quantify the relative standard deviation (RSD%) for the areas associated with trees in each land cover type (Table A1) and for the areas associated with each land cover type between different tree cover data sets (Table A2). The former gives a sense of the magnitude of overall changes and possible errors in the tree cover data sets. The latter defines the areas that are used in our fuel-burned model and therefore gives a sense of possible errors in the data set that we have chosen to use in our analysis (i.e., TC2). Table A3 defines the areas associated with different fractional vegetation cover maps within each land cover type for each region and serves as a measure of the possible errors associated with the data set for vegetation cover that we use in our analysis. These comparisons (Tables A1–A3) are not a perfect measure of error because there may be errors in one or all data sets (owing to the remote sensing method) or because there may be real differences associated with the time of each measurement. Nevertheless, it is instructive to examine these differences.

[82] As shown in Table A1, the tree-covered area detected in TC3 is about 15% smaller overall than that in TC2. It is unlikely that a change of this magnitude is due to a real decrease in tree-cover. Rather, it represents an error in one or both data sets. The tree-covered areas associated with the three different data sets considered here have relative standard deviations that vary from 20 to 79% depending on the region considered and the type of land cover.

[83] Table A2 shows that the differences between the total area in grassland between TC2 and TC3 are similar (within 10% by region), but the differences in area associated with woodlands and with forests is substantial. The TC3 data set has significantly larger areas associated with woodlands and significantly smaller areas associated with forests than does the TC2 data set. Because these land cover types are used in

Table A2. Comparison of Total Area (10^3 km^2 yr^{-1}) in Each Land Cover Type for Different Tree Cover Maps for Each Region

Region	TC1	TC2	TC3[a]	IGBP[b]	Average	RSD, %
			Grasslands, Tc < 40%			
A	11,250	10,883	12,063		11,399	5
B	9945	11,141	11,589		10,892	8
C	11,377	10,440	9510		10,442	9
D	15,741	16,572	15,958		16,090	3
E	18,934	16,505	16,990		17,476	7
F	6967	6997	6218		6727	7
G	7031	6961	7327		7106	3
Total	81,245	79,500	79,655		80,133	1
			Woodlands, 40% < Tc < 60%			
A	2557	1232	2786		2191	38
B	3069	545	1875		1830	69
C	1382	698	1654		1244	40
D	3724	1695	1811		2410	47
E	2555	1259	2853		2222	38
F	1378	728	1623		1243	37
G	384	355	115		285	52
Total	15,049	6511	12,716		11,425	39
			Forests, Tc > 60%			
A	3577	5234	2697	6332	4460	37
B	7489	8807	6586	8043	7732	12
C	1847	3453	1670	3308	2569	37
D	2341	3509	2164	3667	2920	27
E	3217	6940	1948	7225	4832	55
F	2539	3153	2914	6542	3787	49
G	266	363	191	655	369	55
Total	21,275	31,459	18,169	35,773	26,669	31

[a]This analysis used the 3.0.0 version of the TC3 data set.
[b]Sum of broad leaf forests, needle leaf forests, and mixed forests which are defined as having tree cover > 60% in the IGBP land cover map.

Table A3. Comparison of Fractional Vegetation Areas (10^3 km^2 yr^{-1}) for Each Land Cover Type for Different Fractional Vegetation Cover Maps for Each Region

Region	Fc′[a]	Fc[b]	Difference,[c] %	TC3[d]	Difference,[e] %
			Grasslands[f]		
A	8371	8441	−1	9591	14
B	9766	9784	0	10,124	3
C	7136	7161	0	7691	7
D	11,601	11,614	0	12,966	12
E	12,673	12,747	−1	12,747	0
F	4735	4755	0	5592	18
G	4008	4014	0	4633	15
Total	58,291	58,516	0	63,344	8
			Woodlands[f]		
A	2368	2453	−3	2767	13
B	1720	1730	−1	1876	8
C	1489	1510	−1	1654	10
D	1706	1722	−1	1815	5
E	2625	2712	−3	2836	5
F	1409	1434	−2	1625	13
G	94	95	−1	113	19
Total	11,411	11,657	−2	12,685	9
			Forests[f]		
A	2471	2546	−3	2701	6
B	6271	6323	−1	6602	4
C	1568	1590	−1	1674	5
D	1987	2079	−4	2169	4
E	1809	1881	−4	1951	4
F	2643	2716	−3	2921	8
G	174	174	0	191	10
Total	16,924	17,310	−2	18,210	5

[a]Based on *Zeng et al.* [2000].
[b]Calculated from equations (3) and (4).
[c]Percentage difference between *Fc′* and *Fc*.
[d]This analysis used the 3.0.0 version of the TC3 data set.
[e]Percentage difference between the vegetation cover in TC3 and *Fc*.
[f]TC3 was used to classify the land cover type.

our fuel burn model, these changes could represent substantial errors in our method for determining fuel burned in each region. In woodlands only CWD is burned, while in forests CWD, living trees, and SOC in peat areas is burned. Since our fuel model for woodlands also considers cases in which the tree-felled factor and residual smoldering factors are equal to one, these cases partially compensate for these differences in classification of woodlands between these tree cover data sets.

[84] In Table A3 we compare the fractional areas associated with vegetation from the data set developed by *Zeng et al.* [2000], Fc', that calculated from equations (3) and (4) in the text, Fc, and that developed from version 3.0.0 of the TC3 data set [*Hansen et al.*, 2003]. As shown there, differences in the fractional vegetation cover are not large between the Fc and Fc' data sets (1% on a global average basis), but that between Fc and the TC3 data set can be substantial. Because the TC3 data set was developed for a time period during and after that for our analysis, it could not be used to determine the fractional vegetation cover, but these differences may indicate errors in one or both data sets.

[85] Table A4 compares the total area burned that was detected by GBA-2000 in each land cover type for different regions for the different tree cover data sets. The burned areas that are associated with grasslands, woodlands, and forests are substantially different in the different data sets. This comparison emphasizes (as does the comparison in Table A2) the uncertainty that is related to our assumptions for which types of fuel are burned in each land cover type.

Table A4. Comparison of Total Area Burned as Detected by GBA-2000 (10^3 km^2 yr^{-1}) in Each Land Cover Type for Different Tree Cover Maps for Each Region

Region	TC1	TC2	TC3[a]	IGBP[b]	Average	RSD, %
			Grasslands			
A	24	19	31		25	24
B	102	109	123		111	10
C	137	133	139		137	2
D	1518	1789	2085		1797	16
E	208	179	227		205	12
F	68	69	73		70	4
G	517	471	549		513	8
Total	2575	2769	3227		2857	12
			Woodlands			
A	7	5	5		5	29
B	27	5	8		14	87
C	6	5	5		5	18
D	858	353	306		506	61
E	32	19	33		28	27
F	21	8	14		15	42
G	39	64	7		37	78
Total	991	459	379		610	55
			Forests			
A	6	14	2	12	8	68
B	7	22	3	14	11	73
C	7	13	5	13	9	41
D	29	262	15	281	147	98
E	37	79	13	80	52	63
F	4	15	5	16	10	64
G	4	25	3	5	9	118
Total	94	431	46	421	248	83

[a]This analysis used the 3.0.0 version of the TC3 data set.
[b]Sum of broad leaf forests, needle leaf forests, and mixed forests which are defined as having tree cover > 60% in the IGBP land cover map.

Table A5. Comparison of Annual Tree-Covered Area Burned Detected by GBA-2000 (10^3 km^2 yr^{-1}) in Each Land Cover Type for Different Tree Cover Maps for Each Region

Region	TC1	TC2	TC3[a]	Average	RSD, %
		Grasslands			
A	2	1	4	2	50
B	13	3	19	12	67
C	8	2	10	7	58
D	266	155	371	264	41
E	14	6	22	14	58
F	9	4	11	8	49
G	52	32	41	41	24
Total	364	204	479	349	40
		Woodlands			
A	4	2	2	3	30
B	13	3	4	7	86
C	3	2	3	3	17
D	424	176	140	247	63
E	16	10	16	14	25
F	10	4	7	7	41
G	18	31	3	17	80
Total	488	229	175	298	56
		Forests			
A	4	12	1	6	98
B	5	17	2	8	99
C	5	11	4	7	59
D	22	203	10	78	138
E	27	71	9	36	90
F	3	14	3	7	90
G	3	19	2	8	120
Total	69	347	31	149	116

[a]This analysis used the 3.0.0 version of the TC3 data set.

Again, this variation is partially quantified by the consideration of scenarios Sc1–Sc4 for woodlands. Table A5 provides a similar quantification of differences to that in Table A4 but restricts it to only those tree-covered areas which were burned.

[86] **Acknowledgments.** We are grateful to the NASA Global Aerosol Climatology Program and the NASA Radiation Sciences Program and the DOE Atmospheric Chemistry Program for partial support of this work. We thank the European Space Agency-ESA/ESRIN via Galileo Galilei, CP 64, I-00044 Frascati, Italy, for providing the ATSR data and the Joint Research Centre (JSC), Ispra (VA) I-21020, Italy, for providing the GBA-2000 data. The authors wish to thank the Distributed Active Archive Center (code 9020.2) at Goddard Space Flight Center, Greenbelt, MD 20771, for producing the soil type data in its present format and distributing them.

References

Andreae, M. O. (1991), Biomass burning: Its history, use, and distribution and its impact on environmental quality and global climate, in *Global Biomass Burning, Atmospheric, Climatic, and Biospheric Implications*, edited by J. S. Levine, pp. 3–21, MIT Press, Cambridge, Mass.

Andreae, M. O., and P. Merlet (2001), Emission of trace gases and aerosols from biomass burning, *Global Biogeochem. Cycles*, *15*, 966–995.

Andreae, M. O., E. Atlas, H. Cachier, W. R. Cofer III, G. W. Harris, G. Helas, R. Koppmann, J.-P. Lacaux, and D. E. Ward (1996), Trace gas and aerosol emissions from savanna fires, in *Biomass Burning and Global Change*, edited by J. S. Levine, pp. 278–295, MIT Press, Cambridge, Mass.

Araújo, T. M., J. A. Carvalho, N. Higuchi, A. C. P. Brasil, and A. L. A. Mesquita (1999), A tropical rainforest clearing experiment by biomass burning in the state of Pará, Brazil, *Atmos. Environ.*, *33*, 1991–1998.

Arino, O., and J.-M. Melinotte (1998), The 1993 Africa Fire Map, *Int. J. Remote Sens.*, *19*, 2019–2023.

Arino, O., and S. Plummer (Eds.) (2001), *Along Track Scanning Radiometer World Fire Atlas: Validation of the 1997–98 Active Fire Product*, ESA-ESRIN, Frascati, Italy.

Barbosa, P. M., D. Stroppiana, J.-M. Grégoire, and J. M. C. Pereira (1999), An assessment of vegetation fire in Africa (1981–1991): Burned areas,

burned biomass and atmospheric emissions, *Global Biogeochem. Cycles*, *13*, 933–950.

Barrett, D. J. (2002), Steady state turnover time of carbon in the Australian terrestrial biosphere, *Global Biogeochem. Cycles*, *16*(4), 1108, doi:10.1029/2002GB001860.

Batjes, N. H. (1996), Total carbon and nitrogen in the soils of the world, *Eur. J. Soil Sci.*, *47*, 151–163.

Bergamaschi, P., R. Hein, M. Heimann, and P. J. Crutzen (2000a), Inverse modeling of the global CO cycle: 1. Inversion of CO mixing ratios, *J. Geophys. Res.*, *105*, 1909–1927.

Bergamaschi, P., R. Hein, C. A. M. Brenninkmeijer, and P. J. Crutzen (2000b), Inverse modeling of the global CO cycle: 2. Inversion of $^{13}C/^{12}C$ and $^{18}O/^{16}O$ isotope ratios, *J. Geophys. Res.*, *105*, 1929–1945.

Bertschi, I., R. J. Yokelson, D. E. Ward, R. E. Babbitt, R. A. Susott, J. G. Goode, and W. M. Hao (2003a), Trace gas and particle emissions from fires in large diameter and belowground biomass fuels, *J. Geophys. Res.*, *108*(D13), 8472, doi:10.1029/2002JD002100.

Bertschi, I. T., R. J. Yokelson, D. E. Ward, T. J. Christian, and W. M. Hao (2003b), Trace gas emissions from the production and use of domestic biofuels in Zambia measured by open-path Fourier transform infrared spectroscopy, *J. Geophys. Res.*, *108*(D13), 8469, doi:10.1029/2002JD002158.

Brown, S., and G. Gaston (1995), Use of forest inventories and geographic information systems to estimate biomass density of tropical forests: Application to tropical Africa, *Environ. Monit. Assess.*, *38*, 157–168.

Brown, S., L. R. Iverson, A. Prasad, and D. Liu (1993), Geographical distributions of carbon in biomass and soils of tropical Asian forests, *Geocarto Int.*, *4*, 45–59.

Carvalho, J. A., N. Higuchi, T. M. Araújo, and J. C. Santos (1998), Combustion completeness in a rainforest clearing experiment in Manaus, Brazil, *J. Geophys. Res.*, *103*, 13,195–13,199.

Carvalho, J. A., F. S. Costa, C. A. G. Veras, D. V. Sandberg, E. C. Alvarado, R. Gielow, A. M. Serra, and J. C. Santos (2001), Biomass fire consumption and carbon release rates of rainforest-clearing experiments conducted in northern Mato Grosso, Brazil, *J. Geophys. Res.*, *106*, 17,877–17,887.

Crutzen, P. J., and M. O. Andreae (1990), Biomass burning in the tropics: Impact on atmospheric chemistry and biogeochemical cycles, *Science*, *250*, 1669–1678.

DeFries, R., M. Hansen, J. R. G. Townshend, A. C. Janetos, and T. R. Loveland (2000), A new global 1 km data set of percentage tree cover derived from remote sensing, *Global Change Biol.*, *6*, 247–254.

Fearnside, P. M., N. Leal, and F. M. Fearnside (1993), Rainforest burning and the global carbon budget: Biomass, combustion efficiency, and charcoal formation in the Brazilian Amazon, *J. Geophys. Res.*, *98*, 16,733–16,743.

Fearnside, P. M., P. M. L. A. Graça, N. L. Filho, F. J. A. Rodrigues, and J. M. Robinson (1999), Tropical forest burning in Brazilian Amazonia: Measurement of biomass loading, burning efficiency and charcoal formation at Altamira, Pará, *For. Ecol. Manage.*, *123*, 65–79.

Fearnside, P. M., P. M. L. A. Graça, and F. J. A. Rodrigues (2001), Burning of Amazonian rainforests: Burning efficiency and charcoal formation in forest cleared for cattle pasture near Manaus, Brazil, *For. Ecol. Manage.*, *146*, 115–128.

French, N. H. F., E. S. Kasischke, and D. G. Williams (2002), Variability in the emission of carbon-based trace gases from wildfire in the Alaskan boreal forest, *J. Geophys. Res.*, *107*, 8151, doi:10.1029/2001JD000480 [printed 108(D1), 2003].

Fung, I., J. John, J. Lerner, E. Matthews, M. Prather, L. P. Steele, and P. J. Fraser (1991), Three-dimensional model synthesis of the global methane cycle, *J. Geophys. Res.*, *96*, 13,033–13,065.

Gill, R. A., et al. (2002), Using simple environmental variables to estimate below-ground productivity in grasslands, *Global Ecol. Biogeogr.*, *11*, 79–86.

Goode, J. G., R. J. Yokelson, D. E. Ward, R. A. Susott, R. E. Babbitt, M. A. Davies, and W. M. Hao (2000), Measurements of excess O_3, CO_2, CO, CH_4, C_2H_4, C_2H_2, HCN, NO, NH_3, HCOOH, CH_3COOH, HCHO, and CH_3OH in 1997 Alaskan biomass burning plumes by airborne Fourier transform infrared spectroscopy (AFTIR), *J. Geophys. Res.*, *105*, 22,147–22,166.

Graça, P. M. L. A., P. M. Fearnside, and C. C. Cerri (1999), Burning of Amazonian forest in Ariquemes, Rondônia, Brazil: Biomass, charcoal formation and burning efficiency, *For. Ecol. Manage.*, *120*, 179–191.

Grégoire, J.-M., K. Tansey, and J. M. N. Silva (2003), The GBA2000 initiative: Developing a global burned area database from SPOT-VEGETATION imagery, *Int. J. Remote Sens.*, *24*, 1369–1376.

Guild, L. S., J. B. Kauffman, L. J. Ellingson, D. L. Cummings, E. A. Castro, R. E. Babbitt, and D. E. Ward (1998), Dynamics associated with total aboveground biomass C, nutrient pools, and biomass burning of primary forest and pasture in Rondônia, Brazil during SCAR-B, *J. Geophys. Res.*, *103*, 32,091–32,100.

Hansen, M. C., R. S. DeFries, J. R. G. Townshend, and R. Sohlberg (2000), Global land cover classification at 1 km spatial resolution using a classification tree approach, *Int. J. Remote Sens.*, *21*, 1331–1364.

Hansen, M. C., R. S. DeFries, J. R. G. Townshend, R. Sohlberg, C. Dimiceli, and M. Carroll (2002), Towards an operational MODIS continuous field of percent tree cover algorithm: Examples using AVHRR and MODIS data, *Remote Sens. Environ.*, *83*, 303–319.

Hansen, M. C., R. S. DeFries, J. R. G. Townshend, M. Carroll, C. Dimiceli, and R. A. Sohlberg (2003), Global percent tree cover at a spatial resolution of 500 meters: First results of the MODIS vegetation continuous fields algorithm, *Earth Interact.*, *7*(10), 1–15.

Hao, W. M., and M.-H. Liu (1994), Spatial and temporal distribution of tropical biomass burning, *Global Biogeochem. Cycles*, *8*(4), 495–503.

Hao, W. M., M.-H. Liu, and P. J. Crutzen (1990), Estimates of annual and regional releases of CO_2 and other trace gases to the atmosphere from fires in the tropics, based on the FAO statistics for the period 1975–1980, in *Fire in the Tropical Biota: Ecosystem Processes and Global Challenges*, edited by J. G. Goldammer, pp. 440–462, Springer-Verlag, New York.

Harmon, M. E., and C. Hua (1991), Coarse woody debris dynamics in two old-growth ecosystems, *BioScience*, *41*, 604–610.

Heimann, M., and E. Maier-Reimer (1996), On the relations between the oceanic uptake of CO_2 and its carbon isotopes [CO_2], *Global Biogeochem. Cycles*, *10*, 89–110.

Hély, C., K. Caylor, S. Alleaume, R. J. Swap, and H. H. Shugart (2003), Release of gaseous and particulate carbonaceous compounds from biomass burning during the SAFARI 2000 dry season field campaign, *J. Geophys. Res.*, *108*(D13), 8470, doi:10.1029/2002JD002482.

Hoffa, E. A., D. E. Ward, W. M. Hao, R. A. Susott, and R. H. Wakimoto (1999), Seasonality of carbon emissions from biomass burning in a Zambian savanna, *J. Geophys. Res.*, *104*, 13,841–13,853.

Holloway, T., H. Levy II, and P. Kasibhatla (2000), Global distribution of carbon monoxide, *J. Geophys. Res.*, *105*, 12,123–12,147.

Houghton, R. A., K. T. Laurence, J. L. Hackler, and S. Brown (2001), The spatial distribution of forest biomass in the Brazilian Amazon: A comparison of estimates, *Global Change Biol.*, *7*, 731–746.

Hurst, D. F., D. W. T. Griffith, and G. D. Cook (1994a), Trace gas emissions and biomass burning in tropical Australian savannas, *J. Geophys. Res.*, *99*, 16,441–16,456.

Hurst, D. F., D. W. T. Griffith, J. N. Carras, D. J. Williams, and P. J. Fraser (1994b), Measurements of trace gas emitted by Australian savanna fires during the 1990 dry season, *J. Atmos. Chem.*, *18*, 33–56.

Jenkins, J. C., R. A. Birdsey, and Y. Pan (2001), Biomass and NPP estimation for the mid-Atlantic region (USA) using plot-level forest inventory data, *Ecol. Appl.*, *11*, 1174–1193.

Jobbágy, E. G., and R. B. Jackson (2000), The vertical distribution of soil organic carbon and its relation to climate and vegetation, *Ecol. Appl.*, *10*, 423–436.

Kauffman, J. B., D. L. Cummings, and D. E. Ward (1998), Fire in the Brazilian Amazon, 2, Biomass, nutrient pools and losses in cattle pastures, *Oecologia*, *113*, 415–427.

Kicklighter, D. W., et al. (1999), A first-order analysis of the potential role of CO2 fertilization to affect the global carbon budget: A comparison of four terrestrial biosphere models, *Tellus Ser. B*, *51*, 343–366.

Lavoué, D., C. Liousse, H. Cachier, B. J. Stocks, and J. G. Goldammer (2000), Modeling of carbonaceous particles emitted by boreal and temperate wildfires at northern latitudes, *J. Geophys. Res.*, *105*, 26,871–26,890.

Lindesay, J. A., M. O. Andreae, J. G. Goldammer, G. Harris, H. J. Annegarn, M. Garstang, R. J. Scholes, and B. W. van Wilgen (1996), International Geosphere-Biosphere Programme/International Global Atmospheric Chemistry SAFARI-92 field experiment: Background and overview, *J. Geophys. Res.*, *101*(D19), 23,521–23,530.

Liousse, C., J. E. Penner, C. Chuang, J. J. Walton, H. Eddleman, and H. Cachier (1996), A global three-dimensional model study of carbonaceous aerosols, *J. Geophys. Res.*, *101*, 19,411–19,432.

Liski, J., and P. Kauppi (2000), Wood supply and carbon sequestration: Situation and changes, B, Carbon cycle and biomass, in *Forest Resources of Europe, CIS, North America, Australia, Japan and New Zealand (Industrialized Temperate/Boreal Countries): United Nations-Economic Commission for Europe/Food and Agriculture Organization Contribution to the Global Forest Resources Assessment 2000*, pp. 155–171, United Nations, New York.

Lobert, J. M., W. C. Keene, L. A. Logan, and R. Yevich (1999), Global chlorine emissions from biomass burning: Reactive chlorine emissions inventory, *J. Geophys. Res.*, *104*, 8373–8389.

Loveland, T. R., B. C. Reed, J. F. Brown, D. O. Ohlen, J. Zhu, L. Yang, and J. W. Merchant (2000), Development of a global land cover character-

istics database and IGBP Discover from 1 km AVHRR data, *Int. J. Remote Sens.*, *21*, 1303–1330.
Matthews, E. (1983), Global vegetation and land use: New high-resolution data bases for climate studies, *J. Clim. Appl. Meteorol.*, *22*, 474–487.
Matthews, E. (1997), Global litter production, pools, and turnover times: Estimates from measurement data and regression models, *J. Geophys. Res.*, *102*, 18,771–18,800.
Menaut, J. C., L. Abbadie, F. Lavenu, P. Loudjani, and A. Podaire (1991), Biomass burning in west African savannas, in *Global Biomass Burning*, *Atmospheric, Climatic, and Biospheric Implications*, edited by J. S. Levine, pp. 133–142, MIT Press, Cambridge, Mass.
Myneni, R. B., R. R. Nemani, and S. W. Running (1997), Estimation of global leaf area index and absorbed par using radiative transfer models, *IEEE Trans. Geosci. Remote Sens.*, *35*, 1380–1393.
Myneni, R. B., J. Dong, C. J. Tucker, R. K. Kaufmann, P. E. Kauppi, J. Liski, L. Zhou, V. Alexeyev, and M. K. Hughes (2001), A large carbon sink in the woody biomass of northern forests, *Proc. Natl. Acad. Sci. USA*, *98*(26), 14,784–14,789.
National Greenhouse Gas Inventory Committee (NGGIC) (2002), *National Greenhouse Gas Inventory 2000*, Aust. Greenhouse Off., Canberra, ACT.
Olson, J. S. (1994), Global ecosystems framework: Definitions, *Internal Rep.*, U.S. Geol. Surv., EROS Data Cent., Sioux Falls, S. D.
Page, S. E., F. Siegert, J. O. Rieley, H.-D. V. Boehm, A. Jaya, and S. Limin (2002), The amount of carbon released from peat and forest fires in Indonesia during 1997, *Nature*, *420*, 61–65.
Potter, C. S., V. Brooks-Genovese, S. A. Klooster, M. Bobo, and A. Torregrosa (2001), Biomass burning losses of carbon estimated from ecosystem modeling and satellite data analysis for the Brazilian Amazon region, *Atmos. Environ.*, *35*(10), 1773–1781.
Prather, M. J. (1996), Timescales in atmospheric chemistry: Theory, GWPs for CH_4, and CO, and runaway growth, *Geophys. Res. Lett.*, *23*, 2597–2600.
Roads, J. O., et al. (2003), GCIP water and energy budget synthesis (WEBS), *J. Geophys. Res.*, *108*(D16), 8609, doi:10.1029/2002JD002583.
Roy, D. P., P. E. Lewis, and C. O. Justice (2002), Burned area mapping using multi-temporal moderate spatial resolution data—A bi-directional reflectance model-based expectation approach, *Remote Sens. Environ.*, *83*, 263–286.
Russell-Smith, J., A. C. Edwards, and G. D. Cook (2003), Reliability of biomass burning estimates from savanna fires: Biomass burning in northern Australia during the 1999 Biomass Burning and Lightning Experiment B field campaign, *J. Geophys. Res.*, *108*(D3), 8405, doi:10.1029/2001JD000787.
Saket, M. (2001), Wood volume and woody biomass, in *Global Forest Resources Assessment 2000*, edited by A. Perlis, pp. 17–22, Forest and Agric. Org. of the United Nations, Rome.
Schimel, D., D. Alves, I. Enting, M. Heimann, F. Joos, D. Raynaud, and T. Wigley (1996), Radiative forcing of climate change: CO_2 and the carbon cycle, in *IPCC Climate Change: The Science of Climate Change*, edited by J. T. Houghton et al., chap. 2.1, pp. 76–86, Cambridge Univ. Press, New York.
Scholes, R. J., J. Kendall, and C. O. Justice (1996), The quantity of biomass burned in southern Africa, *J. Geophys. Res.*, *101*, 23,667–23,676.
Seiler, W., and P. J. Crutzen (1980), Estimates of gross and net fluxes of carbon between the biosphere and the atmosphere from biomass burning, *Clim. Change*, *2*, 207–247.
Shea, R. W., B. W. Shea, J. B. Kauffman, D. E. Ward, C. I. Haskins, and M. C. Scholes (1996), Fuel biomass and combustion factors associated with fires in savanna ecosystems of South Africa and Zambia, *J. Geophys. Res.*, *101*, 23,551–23,568.
Shirai, T., et al. (2003), Emission estimates of selected volatile organic compounds from tropical savanna burning in northern Australia, *J. Geophys. Res.*, *108*(D3), 8406, doi:10.1029/2001JD000841.
Siegenthaler, U., and J. L. Sarmiento (1993), Atmospheric carbon dioxide and the ocean, *Nature*, *365*, 119–125.
Silva, J. M. N., J. M. C. Pereira, A. I. Cabral, A. C. L. Sá, M. J. P. Vasconcelos, B. Mota, and J.-M. Grégoire (2003), An estimate of the area burned in southern Africa during the 2000 dry season using SPOT-VEGETATION satellite data, *J. Geophys. Res.*, *108*(D13), 8498, doi:10.1029/2002JD002320.
Simon, M., S. Plummer, F. Fierli, J. Hoelzemann, and O. Arino (2004), Burnt area detection at global scale using ATSR-2: The GLOBSCAR products and their qualification, *J. Geophys. Res.*, *109*, D14S02, doi:10.1029/2003JD003622, in press.
Sinha, P., P. V. Hobbs, R. J. Yokelson, I. T. Bertschi, D. R. Blake, I. J. Simpson, S. Gao, T. W. Kirchstetter, and T. Novakov (2003), Emissions of trace gases and particles from savanna fires in southern Africa, *J. Geophys. Res.*, *108*(D13), 8487, doi:10.1029/2002JD002325.
Swap, R. J., H. J. Annegarn, J. T. Suttles, M. D. King, S. Platnick, J. L. Privette, and R. J. Scholes (2003), Africa burning: A thematic analysis of the Southern African Regional Science Initiative (SAFARI 2000), *J. Geophys. Res.*, *108*(D13), 8465, doi:10.1029/2003JD003747.
Tans, P., J. Berry, and P. Keeling (1993), Oceanic $^{13}C/^{12}C$ observations: A new window on ocean CO_2 uptake, *Global Biogeochem. Cycles*, *7*, 353–368.
Tansey, K. (2002), Implementation of regional burnt area algorithms for the GBA-2000 initiative, *Rep. EUR 20532 EN*, Joint Res. Cent., Eur. Commiss., Ispra, Italy.
van der Werf, G. R., J. T. Randerson, G. J. Collatz, and L. Giglio (2003), Carbon emissions from fires in tropical and subtropical ecosystems, *Global Change Biol.*, *9*, 547–562.
Ward, D. E., and L. F. Radke (1993), Emissions measurements from vegetation fires: A comparative evaluation of methods and results, in *Fire in the Environment: The Ecological*, *Atmospheric and Climatic Importance of Vegetation Fires*, edited by P. J. Crutzen and J. G. Goldammer, pp. 53–76, John Wiley, Hoboken, N. J.
Ward, D. E., W. M. Hao, R. A. Susott, R. E. Babbitt, R. W. Shea, J. B. Kauffman, and C. O. Justice (1996), Effect of fuel composition on combustion efficiency and emission factors for African savanna ecosystems, *J. Geophys. Res.*, *101*, 23,569–23,576.
Waring, R. H., J. J. Landsberg, and M. Williams (1998), Net primary production of forests: A constant fraction of gross primary production?, *Tree Physiol.*, *18*, 129–134.
Warneck, P. (1988), *Chemistry of the Natural Atmosphere*, Academic, San Diego, Calif.
Yevich, R., and J. A. Logan (2003), An assessment of biofuel use and burning of agricultural waste in the developing world, *Global Biogeochem. Cycles*, *17*(4), 1095, doi:10.1029/2002GB001952.
Yokelson, R. J., I. T. Bertschi, T. J. Christian, P. V. Hobbs, D. E. Ward, and W. M. Hao (2003), Trace gas measurements in nascent, aged, and cloud-processed smoke from African savanna fires by airborne Fourier transform infrared spectroscopy (AFTIR), *J. Geophys. Res.*, *108*(D13), 8478, doi:10.1029/2002JD002322.
Zeng, X., R. E. Dickinson, A. Walker, M. Shaikh, R. S. DeFries, and J. Qi (2000), Derivation and evaluation of global 1-km fractional vegetation cover data for land modeling, *J. Appl. Meteorol.*, *39*, 826–839.
Zhu, Z., and E. Waller (2001), FRA 2000 global forest cover mapping final report, *For. Resour. Assess. Prog. Working Pap. 50*, edited by P. Pugliese, For. and Agric. Org. of the United Nations, Rome.
Zobler, L. (1986), A world soil file for global climate modeling, *NASA Tech. Memo. 87802*, 33 pp., Greenbelt, Md.

A. Ito and J. E. Penner, Department of Atmospheric, Oceanic and Space Sciences, University of Michigan, 2455 Hayward, Ann Arbor, MI 48109-2143, USA. (penner@umich.edu)